TOWSON UNIVERSITY
OFFICE OF GRADUATE STUDIES

DETECTING SPATIO-TEMPORAL CHANGES IN BALTIMORE, MARYLAND'S HEAT ISLAND WITH REMOTE SENSING IMAGERY

by

Sara H. Levy

A thesis

Presented to the faculty of

Towson University

in partial fulfillment

of the requirements for the degree

Master of Arts

Department of Geography and Environmental Planning

Towson University
Towson, Maryland 21252

May 2016

TOWSON UNIVERSITY
OFFICE OF GRADUATE STUDIES

THESIS APPROVAL PAGE

This is to certify that the thesis prepared by Sara H. Levy, entitled DETECTING SPATIO-TEMPORAL CHANGES IN BALTIMORE, MARYLAND'S HEAT ISLAND WITH REMOTE SENSING IMAGERY has been approved by the thesis committee as satisfactorily completing the thesis requirements for the degree Master of Arts.

Dr. Todd Moore, Chair, Thesis Committee	Date 4/13/2016
Dr. John Morgan, Committee Member	Date 4/13/16
Dr. Martin Roberge, Committee Member	Date 4/13/16
Janet V. DeLany, Dean Graduate Studies Dean of Graduate Studies	4/29/16 Date

ACKNOWLEDGEMENTS

This thesis would not have been accomplished without the support of many and I owe my gratitude to all those who made this research possible and because of whom my graduate experience has been one that I will treasure forever. Foremost, I would like to express my sincere appreciation to Dr. Todd W. Moore, my committee chair for his continued support and encouragement and for helping me sort out the analytical and technical procedures of this thesis. I am also grateful to Dr. John Morgan III and Dr. Martin Roberge for providing me with this opportunity along with expanding my knowledge that allowed me complete this research.

Finally I would like to thank my parents for always believing in me, for always supporting my dreams, and assisting in any way possible. I would also like to specifically thank them both for taking on responsibility with regards to caring for Theodore, my adorable little dog. I would also like to thank my sister for always setting my parents standards high thereby providing me with the determination and motivation needed to complete this thesis.

Thank you.

ABSTRACT

DETECTING SPATIO-TEMPORAL CHANGES IN BALTIMORE, MARYLAND'S HEAT ISLAND WITH REMOTE SENSING IMAGERY

Sara H. Levy

In the past century alone, society has continued to develop and urbanize, making research of the urban heat island (UHI) more important than ever. UHIs have a detrimental impact on human health and the natural environment as a result of increased land surface temperature, changes in precipitation patterns, and other weather related events. This study sought to determine the change and extent of Baltimore, Maryland's UHI with Landsat 5 imagery. Imagery was collected in approximately 5 year intervals from 1985 to 2011 in order to determine how albedo, normalized difference vegetation index (NDVI), land cover, and land surface temperature (LST) changed during each time period. This study found no correlation between change in albedo and change in LST, a slightly negative correlation between change in NDVI and LST, and a positive correlation between land cover and LST in Baltimore's UHI. This study also found that weather, particularly precipitation events occurring prior to the date the satellite image was captured, may have affected the analysis of extent and intensity of Baltimore's UHI.

TABLE OF CONTENTS

LIST OF FIGURES

ABBREVIATIONS

NDVI	Normalized Difference Vegetation Index
LST	Land Surface Temperature
UHI	Urban Heat Island

CHAPTER 1

INTRODUCTION

In the past century, the world has experienced exponential population growth along with rapid urbanization and development. While only 30 percent of the world's population lived in urban areas in 1950, it is projected that approximately 66 percent of the world's population will be living in urban areas by 2050 (United Nations, 2014). North America in particular is one of the most urbanized regions of the world with approximately 82 percent of its population living in urban areas in 2014, followed by Latin America and the Caribbean with 80 percent, and Europe with 73 percent (United Nations, 2014). Rapid urbanization and development has resulted in increased environmental vulnerability due to the depletion of natural resources and has been associated with detrimental impacts on human health and the natural environment through its contribution to increased temperatures within urban and developed areas, as well as to changes in precipitation (Lo *et al.,* 1997; Liu and Zhang, 2011).

Most people think of global climate change, or changes in the Earth's overall climate, when hearing the term *climate change*. Local climate change, or changes in the climate of smaller geographic areas such as cities also is a part of climate change. Some benefits of studying local climate change includes the ability to investigate the causes of climate change, to investigate its impacts and the extent of its impacts, and to search for solutions. This is especially important as many mitigation and adaption strategies occur at the local rather than global scale. For instance, in 2009, Baltimore launched The Baltimore Sustainability Plan in order make Baltimore a more sustainable city and to utilize sustainability elements in the city's planning and development. The plan proposed to

reduce Baltimore's greenhouse gas emissions by 15% by 2015 and double Baltimore's tree canopy by 2037 (Baltimore Commission on Sustainability, 2009).

Urban Heat Islands (UHI) are a prime example of not only local climate change but also how anthropogenic forces can influence climate. UHI's are defined as urban areas with higher land surface and air temperatures than their surrounding non-urban and rural areas (Oke, 1995; Stathopoulou *et al.*, 2005; George *et al.*, 2003; Zhang *et al.*, 2008 Ahmed *et al.*, 2013;). Such increases result from the replacement of natural green vegetation with urban surfaces, including impervious surfaces. Impervious surfaces cause increased water runoff, thereby resulting in less surface water for evapotranspiration (Johnson, 2004; Effat and Hassan, 2014). This can affect the surface energy balance (Grimmond and Oke, 1991; Effat and Hassan, 2014). In addition to changes in land cover, the geometric formation of urban areas, and increased heat waste and emissions within an urban area, contribute to UHIs (Stathopoulou *et al.*, 2005; Ahmed *et al.*, 2013).

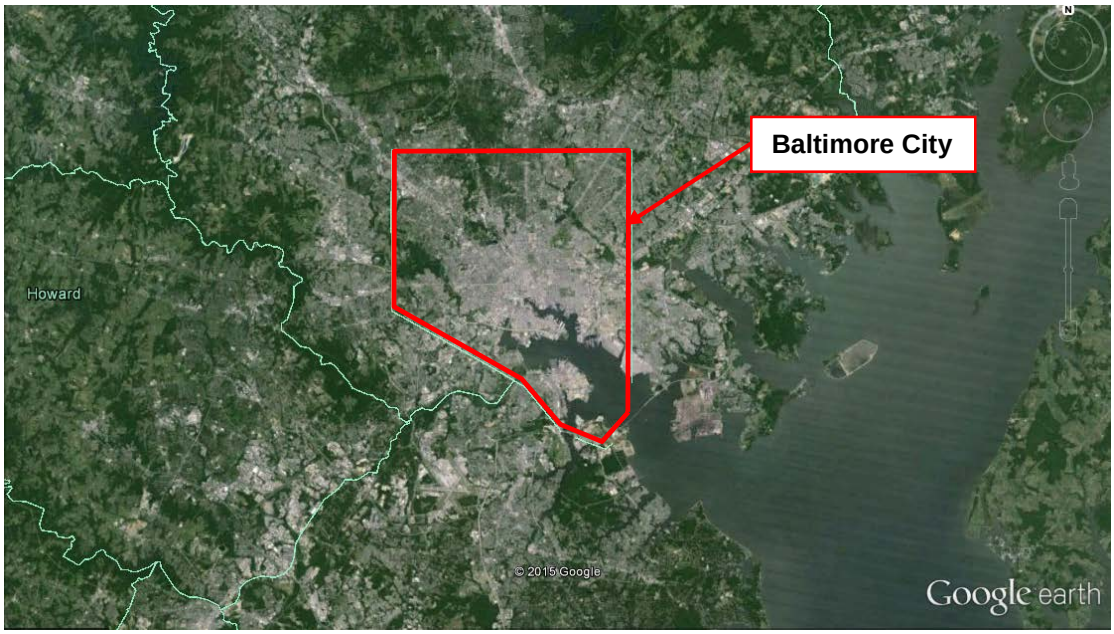

Figure 1.1. Map of the Baltimore City and surrounding areas. Source: Google Earth™ - Image from Landsat

Goals and Objectives

The goal of this study is to detect the spatial and temporal changes in Baltimore's UHI and to find the causes of these changes. It is also the goal to use this study, in conjunction with other applicable UHI studies, to search for solutions for heat stressed environments, and determine appropriate planning for current and future urban development. The objectives for this project were to:

- Map land cover changes in Baltimore
- Map albedo changes in Baltimore
- Map NDVI changes in Baltimore
- Map LST changes in Baltimore
- Analyze the relationships between the aforementioned changes in land surface properties

Delimitations

This study includes the following delimitations:

- Land cover, and LST will be assessed for six time periods resulting in five maps of change detection. The time periods that will be compared are 1985, 1990, 1996, 2000, 2005, and 2011.
- The study will focus solely on Baltimore City and the immediate surrounding area (see Figure 3.1).
- Only Landsat 5 Thematic Mapper imagery captured during anniversary dates in 1985, 1990, 1996, 2006, and 2011 will be used for the project.

Definitions

For this study, the following key terms are defined:

Anniversary images – Images that are captured on the same date and time, or as close to the same date and time as possible. The purpose of using anniversary images is to reduce the effects seasonal changes and changes related to the time of day.

Landsat 5 Thematic Mapper – Landsat 5 TM was initially launched by the National Air and Space Administration (NASA) and was since operated by the U.S. Geological Survey (USGS). Landsat 5 TM was in commission from March 1, 1984 until it was January 2013. Images collected from Landsat 5 TM are approximately 30 meters in resolution, and are comprised of seven spectral bands, and one thermal band (Band 6) (USGS, 2014).

Spatial resolution – A measure of how visible an image is. High resolutions allow for greater accuracy and finer details (Campbell, 2002; Morgan, 2014).

Spectral resolution – The ability of a satellite sensor to detect different wavelengths (Campbell, 2002; Morgan, 2014).

CHAPTER 2

LITERATURE REVIEW

UHIs have been studied since at least 1833, when they were first described by Luke Howard (Liu and Zhang, 2011; Ahmed *et al.,* 2013). Since that time, society has continued on a path of rapid urbanization and development, making research of UHIs more important than ever. UHIs have been related to numerous detrimental impacts on human health and the natural environment (Liu and Zhang, 2011) through their contribution to increased temperatures within urban and developed areas, as well as to changes in precipitation (Lo *et al.,* 1997). An UHI is defined as an environmental phenomenon in which atmospheric and surface temperature within an urban area is greater than the atmospheric and surface temperature in the surrounding non-urban and rural areas (George *et al.,* 2003; Stathopoulou *et al.*, 2005; Zhang *et al.,* 2008; Ahmed *et al.,* 2013). Continued research has expanded the definition of an UHI to include various layers of the atmosphere, various surfaces, and even the subsurface (Oke, 1982, 1995; Voogt and Oke, 1997, 2003; Effat and Hassan, 2014). The extent and intensity of an UHI depends on multiple factors, including the season, time of day, weather conditions, and geographic location. It is important to study UHIs as they provide insight into the causes of local and global climate change and the impacts and extent of UHIs. Additionally, studying UHIs can provide key information to urban planners, natural resource managers, and policymakers to mitigate the effects of UHIs and search for solutions.

Causes of the Urban Heat Island

UHIs are caused by several factors, the most notable being alterations of the Earth's surface brought on by urban development. During urban development, soil and natural

green vegetation are replaced with impervious urban surfaces such as asphalt and concrete, and with urban structures (Akbari, Pomerantz, and Taha, 2001; Voogt and Oke, 2003; Zhou, Huang, and Cadenasso, 2011). These urban surfaces change the albedo, thermal capacity, heat conductivity, and perviousness of the Earth's natural surface (Voogt and Oke, 2003; George *et al*., 2003; Johnson, 2004; Liu and Zhang, 2011; Ahmed *et al.*, 2013; Effat and Hassan, 2014).

Impervious urban surfaces contribute to the UHI effect by not allowing for the natural infiltration of water. Runoff water is able to drain quickly instead of being absorbed by the surface. This leaves less water at the surface for evapotranspiration, thereby affecting the net radiation of the surface (Grimmond and Oke, 1991; Effat and Hassan, 2014). As less energy is used for evapotranspiration in urban areas, the additional energy can be used to heat the surface. Natural soil and vegetation, on the other hand, have the opposite effect of impervious urban surfaces as they are able to retain moisture. These areas allow for evapotranspiration to occur and can even have a cooling effect on the environment (Effat and Hassan, 2014).

Changes in albedo and the thermal capacity of the Earth's surface also contribute to the UHI effect. Urban surfaces such as roads and rooftops tend to have lower albedos than natural surfaces (Effat and Hassan, 2014), therefore less solar radiation is reflected from the Earth's surface. This difference over an entire urban area contributes to changes in the energy balance. In addition, urban surfaces tend to have higher thermal capacities which allows them to store heat during the day, and then release it at night (Effat and Hassan, 2014).

The geometric formation, or the configuration of urban areas, also plays a role in the UHI effect. Urban structures, such as buildings of various sizes and densities, and narrow streets are able to influence local wind patterns and trap urban emissions (Stathopoulou *et al.,* 2005; Ahmed *et al.,* 2013).

Increased population within an urban area also significantly contributes to the UHI effect (Stathopoulou *et al.,* 2005; Ahmed *et al.,* 2013). An increased population results in increased anthropogenic emissions through increases in the power demand, power generation, transportation emissions and emissions from industries. Anthropogenic emissions within an urban area include greenhouse gases and ozone precursors, which can increase tropospheric ozone. When tropospheric ozone is increased, the troposphere has a greater ability to absorb the thermal radiation emitted by the Earth's surface, thereby enhancing the UHI effect (George *et al.,* 2003; Effat and Hassan, 2014).

Remote Sensing of the Urban Heat Island

As early as the 1970s, researchers started using airborne and satellite remote sensing data to identify UHIs based on LSTs (Liu and Zhang, 2011; Ahmed *et al.,* 2013). Prior to the use of satellites, UHIs were studied using ground-based observations that were taken from either vehicle traverses or fixed thermometer networks (Voogt and Oke, 1998; Effat and Hassan, 2014). There are many advantages from using remotely sensed data. They allow the monitoring of LSTs and changes in land cover over time, and provide medium-resolution images that cover a wide geographic area (Stathopoulou *et al.,* 2005; Liu and Zhang, 2011; Ahmed *et al.,* 2013). Remotely sensed thermal wavelengths can provide minimum and maximum temperatures of a geographic area along with spatial patterns of the UHI (Johnson, 1999; Effat and Hassan, 2014). UHI research has utilized

data from satellites such as the AVHRR, ASTER, Landsat Thematic Mapper (Landsat 5 TM), and the Landsat Enhanced Thematic Mapper Plus (ETM+).

One thread of UHI research focuses on developing techniques to measure LST from remotely sensed imagery (George *et al*., 2005*;* Liu and Zhang, 2011; Ahmed *et al.*, 2013*)*. Some of these methods include the split-window method, temperature/emissivity separation method, the mono-window method, and the single-channel method (Liu and Zhang, 2011). The type of available data determines the method used for a specific study. For instance, remotely sensed imagery from Landsat TM is more limited than ASTER data, because the images contain only one thermal band rather than five.

Many factors are involved in determining LST from a remotely sensed image. For instance, before LST can be derived from an image, the image must be geocorrected and corrected radiometrically. Once this is done, the digital number (DN) values must be converted to radiance, which is then converted to brightness temperature. Lastly, brightness temperature is converted to LST after it is corrected for emissivity (Liu and Zhang, 2011).

Another thread of UHI research examines the relationship between LST and land cover composition (e.g. Weng, Lu, and Schubring, 2004; Frey, Rigo, and Parlow, 2007; Weng, 2009; Buyantuyev and Wu, 2010). These studies have shown that land cover and the characteristics of the Earth's surface significantly impact the LST in urban environments (Liang and Weng, 2003; Weng, 2003; Weng *et al*., 2004, Zhou *et al.*, 2011; Effat and Hassan, 2014). For example, Effat and Hassan (2014) looked at the association between albedo and LST for Cairo City, Egypt. The study found that land cover classes with higher albedos typically had less available energy for heat fluxes while areas with

lower albedos, such as built-up areas, had more available energy. There were however, areas with high albedos, such as the desert class, that still had high LSTs.

Other studies developed techniques to measure LST, identify land use/land cover, or calculate normalized difference indices from remotely sensed imagery (Weng, 2001; Sobrino *et al.*, 2004; Zhang, 2008a). The techniques most frequently used to determine land cover include supervised classification, unsupervised classifications, and the use of the normalized vegetation difference index (NDVI) (Weng, 2001; Sobrino *et al*, 2004; Zhang, 2008a). Less common techniques include the normalized difference bareness index (NDBaI), normalized difference built up index (NDBI), and the normalized difference water index (NDWI) (Chen, 2006).

Rinner and Hussain (2011), for instance, determined that a positive relationship exists between NDBI and LST. The study noted that LST was greater in areas used for commercial and industrial purposes and lower in other areas. In addition, Chen *et al*. (2006) determined that there was a negative correlation between NDVI and LST and a positive correlation between NDBI and LST. In their study, increased green vegetation and less development resulted in lower LST, while decreased green vegetation and increased development resulted in higher LSTs.

Spatial-Temporal Changes of UHIs

Previous studies have also focused on the spatial and temporal characteristics of UHIs by comparing two or more remotely sensed images (He *et al.*, 2007; Liu, 2009; Effat and Hassan, 2014). UHIs can change in their extent and intensity based on the time period studied, the time of day, the time of year, the wind conditions present, the UHI's geographic location, among other factors (Imhoff *et al.*, 2010; Zhang *et al.*, 2011; Effat

and Hassan, 2014). They are typically strongest at night, during winter, and under weaker wind conditions, and typically increase in extent and intensity over time (Ahmed *et al.*, 2013).

A study focused on Shanghai, China's UHI revealed that, in a period of only seven years (between 1997 and 2004), a time when Shanghai experienced rapid urbanization and economic growth, the extent and the intensity of Shanghai's UHI increased. A closer look at the growth determined that there was significant spatial patterning present within the UHI between 1997 and 2004 (Li *et al.*, 2009). The results showed that in urbanized and urbanizing areas, homogenous patches dominated and significantly increased, as did the magnitude and extent of the hot spots (Li *et al.*, 2009).

Spatial differences within an UHI were also noted for Cairo City, Egypt's UHI (Effat and Hassan, 2014). Cairo City, for the period studied, experienced rapid urbanization and growth (Effat and Hassan, 2014). The eastern portion of the city, which consists of desert and bare lands had the greatest UHI intensity, while the western portion of the city had the weakest. Although it was determined that the areas with greatest temperatures were bare land over the desert, urban materials such as metal roofs and asphalt strongly contribute to the creation of micro-urban heat islands (Effat and Hassan, 2014).

The geographic location of an UHI significantly affects its extent and intensity as it changes factors such as the type of biome present, wind patterns present, and the proximity to water (Imhoff *et al.*, 2010; Effat and Hassan, 2014). For instance, the weaker UHI intensity in the western portion of Cairo City was attributed to its geographic location, primarily its proximity to the Nile River. Changing from natural surfaces to

urban surfaces creates an UHI, but the extent and intensity is also contingent upon what surface is being replaced. Differences for displacing forests are greater than for temperate grassland and for tropical grasslands and savannas (Imhoff *et al.*, 2010). Urbanized areas forming in deserts, on the other hand, tend to have little to no change in comparison to their non-urban surroundings (Imhoff *et al.*, 2010). The change from desert to urban development can even, at times, have a cooling effect due to increased irrigation which can increase evapotranspiration at the surface (Brazel *et al.*, 2000).

Remote Sensing Studies of the Baltimore region

Although there is extensive research on UHIs, only a handful of studies focus on Baltimore, Maryland's UHI. Prior UHI research in the Baltimore metropolitan area has focused on the effects of neighboring Washington, D.C.'s UHI on Baltimore's UHI (Zhang *et al.*, 2011), the effects of land cover configuration on Baltimore's UHI (Zhou *et al*., 2011), and the socio-economic characteristics of Baltimore's UHI (Huang *et al.*, 2011). Additional studies have compared Baltimore's UHI to Phoenix's UHI and to other cities within the continental United States (Brazel *et al.*, 2000; Imhoff *et al.*, 2010).

Baltimore's geographic location and its configuration has significantly affected its LST along with its UHI extent and intensity. Zhou *et al.* (2011), for instance, studied the effects of both composition and configuration of land cover features in the Gwynns Falls watershed of Baltimore, Maryland. Their study used correlation analysis and multiple linear regression models to determine that composition as well as configuration of land cover features within the watershed significantly impacted LST. Their study also determined that the percentage cover of buildings in Baltimore had the most impact on

LST in a positive direction, while green areas, particularly woody vegetation, is the most important in mitigating the effects of the UHI (Zhou *et al.*, 2011).

Geographically, Baltimore is located along the eastern coast of the United States within a temperate broadleaf and mixed forest biome. Because of this, land cover changes in Baltimore have significantly impacted the magnitude of its UHI especially when compared to desert urban areas such as Phoenix, Arizona and Las Vegas, Nevada. Baltimore's UHI is well-defined and has an amplitude of 9.3ºC compared to Las Vegas' UHI which alludes to a possible heat sink (Imhoff *et al.,* 2010). The NDVI difference between Baltimore's urban core and the surrounding rural areas is 0.4 compares to less than 0.1 for that of Las Vegas (Imhoff *et al.,* 2010). Such differences are also shown through the comparison of Baltimore's UHI to Phoenix's UHI, in which daytime temperatures in Phoenix's UHI tended be cooler than the surrounding rural desert areas. Both cities, however, experienced decreases over time in the temperature difference between urban areas and the surrounding non-urban areas (Brazel *et al.,* 2000).

While previous studies have looked at Baltimore's UHI (Brazel *et al.*, 2000; Imhoff *et al.,* 2010; Zhang *et al.*, 2011; Zhou *et al.,* 2011), none have studied its change over time. Other studies (Chen *et al.,* 2006; Ahmed *et al.,* 2013; Effat and Hassan, 2014), however, have shown that UHIs change in extent and intensity over time in response to land cover changes. This study will aim to determine how Baltimore's UHI has changed over time, and will assess the relationship between land cover, albedo, and NDVI changes to changes in LST.

CHAPTER 3

RESEARCH METHODS

Study Area

Located on the east coast approximately 50 miles north of Washington, D.C. and 90 miles south of Philadelphia, Baltimore, Maryland is the largest independent city in the United States, and the largest city in Maryland. The city is located between 38.7169º and 39.2358ºN latitude and 76.8413º and 76.3486ºW longitude (MSGIC, 2008) and is bordered to the north, east, and west by Baltimore County, to the south by Anne Arundel County to the south-southeast by the Chesapeake Bay (Figure 3.1). The city is located along the fall line, which separates the Piedmont Plateau and the Atlantic Coastal Plain physiographic provinces.

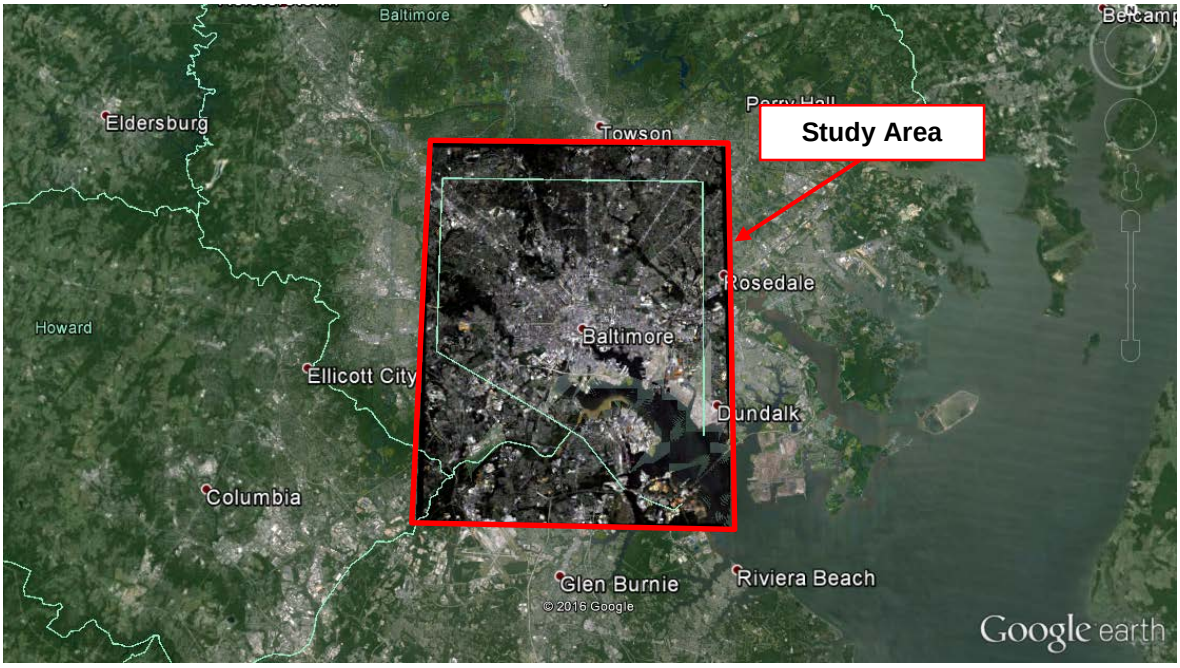

Figure 3.1. Map of the Study Area. Source: Google Earth™ - Image from Landsat

Data Collection

This study used data from Landsat Thematic Mapper (TM) (Landsat5) obtained from the U.S. Geological Survey (USGS) EarthExplorer website (http://earthexplorer.usgs.gov/). EarthExplorer provides online search, browse display, metadata export, and data download for earth science data from USGS archives. Images collected were cloud-free (or as close as possible) and cover anniversary dates spanning several decades.

Once downloaded, the .gzip file from EarthExplorer was extracted using 7-Zip (http://www.7-zip.org/), an open source software application for packing and unpacking compressed files. Pixels in each image measured 30 meters east-west by 30 meters north-south. The following are the map extents and number of rows and columns for the study area:

Upper Left Corner	(39.85114, -78-34761)
Upper Right Corner	(39.89842, -75.49365)
Lower Left Corner	(37.88629, -78.25660)
Lower Right Corner	(37.93039, -75.48020)

Number of Columns: 1817 Number of Rows: 2153

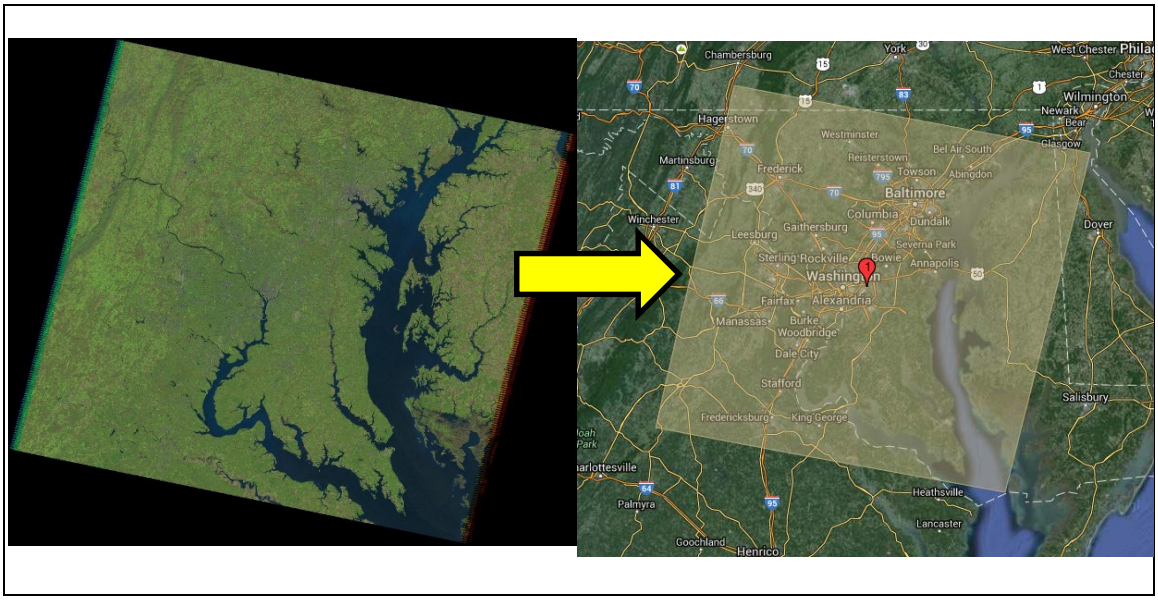

Figure 3.2. Project area and its regional context

Seven Landsat 5 images were analyzed in this study (Table 3.1). Each image met the following criteria:

1. They were captured during summer months June, July, or August.
2. They had less than 10% cloud cover, with no cloud cover in the study area.

Table 3.1: Metadata for Landsat 5 Images

Image ID	Year	Month	Day	Time	Zenith	% Cloud Cover
LT50150331985226XXX10	1985	8	14	15:16:06.9610060Z	54.48201508	0.00
LT50150331990224XXX04	1990	8	12	15:06:26.0100130Z	53.35059695	0.00
LT50150331996193XXX02	1996	7	11	15:00:38.5210380Z	57.19058680	0.00
LT50150332000188AAA02	2000	7	6	15:23:15.8420750Z	61.61908882	0.00
LT50150332005217GNC01	2005	8	5	15:34:25.7280000Z	59.07414694	2.00
LT50150332009196GNC02*	2009	7	15	15:35:17.9830750Z	62.67062235	0.00
LT50150332011234EDC00	2011	8	22	15:35:13.8790440Z	55.56940354	6.00

*The 2009 image is incorporated into the Discussion (Chapter 5).

Pre-Processing

The images were pre-processed by the USGS and are geometrically corrected and geo-referenced to WGS 1984 and Universal Transverse Mercator (UTM) zone 18 N coordinate system. As the seven images collected for this study contain zero percent cloud

cover, no atmospheric correction was applied. In order to identify accurate boundaries for the area of interest, Baltimore City, the image was clipped using the Window function in TerrSet. The extent of Baltimore City is covered in Path 15 Row 33, therefore no additional pre-processing was required.

Classifying Land Cover

This study used a Semi-Supervised Classification in order to determine land cover for each of the images. In this process Bands 1 through 7 were processed using the ISOCLUST function in TerrSet. The ISOCLUST function is based on a similar concept to the ISODATA routine of Ball and Hall (1965) and other cluster routines such as the H-Means and K-Means processes (TerrSet Manual). In this process a specified number of clusters were revealed and then manually grouped together into the desired land cover classes. The images were classified into three following three categories: urban/developed (1) green/non-developed (2) and water (3).

Detecting Changes in Albedo

Albedo is the reflectivity of the Earth's surface. It is the amount of solar energy or shortwave radiation that is reflected rather than absorbed by the surface (Effat and Hassan, 2014; NASA, 2015). Unlike natural green vegetation, urban areas are built up and consists of surfaces with generally low albedos, and higher impermeability (Effat and Hassan, 2014). The albedo for the Landsat images used for this study was determined using the formula presented by Liang (2000) (Equation 1). This formula was normalized by Smith (2010) in order to calculate shortwave radiation, and was used in Effat (2014).

$$Albedo = \frac{[(0.356 * B1) + (0.130 * B2) + (0.373 * B3) + (0.085 * B4) + (0.072 * B5) - 0.018]}{1.016}$$

*Source: Effat, 2014; Liang, 2000; Smith, 2010

Equation 1

Deriving the Normalized Difference Vegetation Index

NDVI is a vegetation index extensively used to assess, or measure, vegetation greenness or photosynthetic activity (Chen *et al.,* 2004; Wang *et al.,* 2004; Chen *et al.,* 2006). Many UHI studies have found a correlation between NDVI and LST (Chen *et al.,* 2006, Liu and Zhang, 2011). Liu and Zhang (2011), for instance, found a negative correlation between NDVI and LST, while Chen *et al.* (2006) found a negative correlation up until NDVI reached 0.6 when the correlation became a positive linear correlation.

NDVI was calculated for each of the images using Equation 2, which does a ratio calculation of the near infrared band (Band 4 in Landsat TM), and the red band (Band 3 in Landsat TM). Greater NDVI values indicate healthy vegetation, while lower values indicate stressed vegetation or other land cover (Liu and Zhang, 2011; Morgan, 2014).

$$\text{NDVI} = \frac{\text{NIR band} - \text{VR band}}{\text{NIR band} + \text{VR band}}$$

*Source: Morgan, 2014; Sobrino *et al.,* 2004; Liu and Zhang, 2011

Equation 2

Deriving Land Surface Temperature from Landsat Thermal Band

Land Surface Temperature and Temperature Maps

The final temperature maps for each of the images were created using the TerrSet IDIRSI Thermal Function, which converts data values in Landsat TM Band 6 (TIR) to blackbody temperatures (Eastman, 2012). By doing so, the process follows the steps mentioned below; however, it is up to the user to create the emissivity band. This study corrected for emissivity based on the process presented in Section 3.6.3. The temperature values for this study were calculated for Landsat 5 images in degrees Fahrenheit.

Converting Digital Numbers (DN) to Spectral Radiance Values

Deriving LST from a Landsat TM image required further pre-processing, as there are additional factors to consider. The next step in pre-processing required the conversion from DN to radiance values. The thermal infrared band (Band 6) consists of 8-bit data with DN that range from zero to 255 (256 total). Conversion was completed using Equation 3 as shown below:

$$CV_R = G(CV_{DN}) + B$$

CV_R = cell value as radiance
CV_{DN} = cell value as digital number
G = gain (0.005632156 for TM)
B = offset (0.1238 for TM)

*source: Bhamare and Agone, 1990

Equation 3

Converting Spectral Radiance Values to Brightness Temperatures

Once the radiance values were calculated, they were converted to brightness temperatures using Plank's inverse function. Brightness values, however, are not an

accurate representation of LST but rather a “mixed signal or the sum of different fractions of energy” (Yang and Wang, 2002, 2). This is because they “include the energy emitted from the ground, upwelling radiance from the atmosphere, as well as the down welling radiance from the sky integrated over the hemisphere above the surface” (Yang and Wang, 2002, 2). Plank’s inverse function is denoted by Equation 4:

$$T = \frac{K_2}{\ln\left(\frac{K_1}{CV_R} + 1\right)}$$

T = degrees Kelvin
CV_R = cell value as radiance
K_1 = calibration constant 1 (607.76 for TM)
K_2 = calibration constant 2 (1260.56 for TM)

*Source: Zhang *et al.,* 2008

Equation 4

Estimating Emissivity from the Normalized Difference Vegetation Index

The next step was to account for the emissivity within the Landsat TM images in order to acquire accurate LST. Several methods have been developed to determine the emissivity of an image. This study utilized the emissivity estimation method presented by Zhang (2006), which utilizes NDVI values for an image (Liu and Zhang, 2011). NDVI values were converted to land surface emissivity values according to Table 3.2 through the RECLASS function and Image Calculator in TerrSet.

Table 3.2. Land surface emissivity values based on NDVI values.

NDVI	Land Surface Emissivity
NDVI < -0.185	0.995
-0.`85 ≤ NDVI < 0.157	0.970
0.157 ≤ NDVI ≤ 0.727	1.0094 + 0.04ln(NDVI)
NDVI > 0.727	0.990
*Source: Liu, 2011	

Deriving Land Surface Temperature

Once emissivity was calculated, land surface temperature were derived from the Landsat image using Equation 5:

$$S_t = \frac{T}{1 + (\lambda + T/\rho)\ln \varepsilon}$$

S_t = land surface temperature
ƛ = wavelength of emitted radiance
ρ = h*c/σ (1.438 * 10^{-2} m K)
σ = Boltzman constant (1.38 * 10^{-23} J/K)
h = Planck's constant (6.626 * 10^{-34} J/s)
c = velocity of light (2.998 * 108 m/s)

*Source: Bhamare and Agone, 1990; Zhang *et al.*, 200*8*

Equation 5

Change Detection

Change detection was determined through the Image Calculator function in the IDRISI GIS Analysis portion of TerrSet. Each image was subtracted from the newer image in order to determine the difference between the two images. For instance, the 2005 LST

map was subtracted from the 2011 LST map to determine the overall change in LST between the two images. This process was applied to albedo, NDVI and LST. Change in land cover, however, was determined by comparing the areas (given in number of pixels) for each cover for each year using the AREA function in TerrSet.

CHAPTER 4

RESULTS

Land Surface Temperature 1985-2011

LST maps were generated for 1985, 1990, 1996, 2000, 2005, and 2011 (Figure 4.1). In 1985, LST appears to be greatest in the downtown area of Baltimore City where urban development is the greatest. Temperatures in this area contain a mixture of 85º to 90ºF, and 90º to 100ºF. As you move outward from the central portion of the city, temperature decreases to a mix of 90º to 95ºF, along major roadways and suburban development, and 80º to 85ºF. Areas between 70º to 75ºF are noted in the southeast portion of the city, where the Patapsco River (water) is, and in areas in the southwest, the west, and northwest, where forested areas are. This pattern is also present in the 1990, 1996, 2000, 2005, and 2011 images (Figure 4.1); however to varying degrees. Temperatures appear to be greatest in the downtown portion of Baltimore City and decrease farther out towards less urbanized areas. Major roadways, most notably Route 1 and Interstate 95 (I-95) in the northeastern portion of the study area, also appear to be very warm in the images. The coolest areas consist of the known forested areas (in the southwestern portion and western portion of Baltimore), and the Patapsco River (southeastern portion of the image).

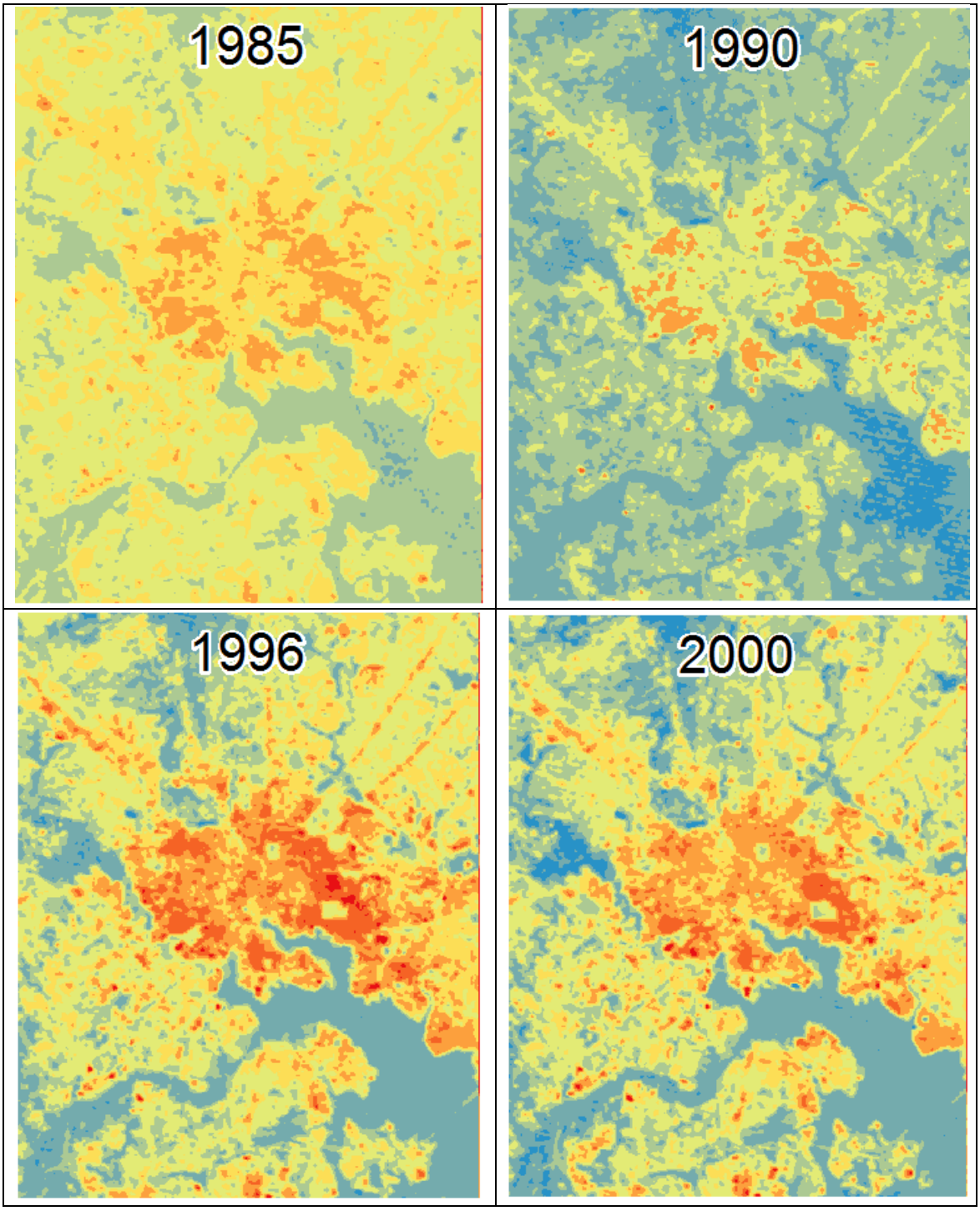
1985
1990
1996
2000

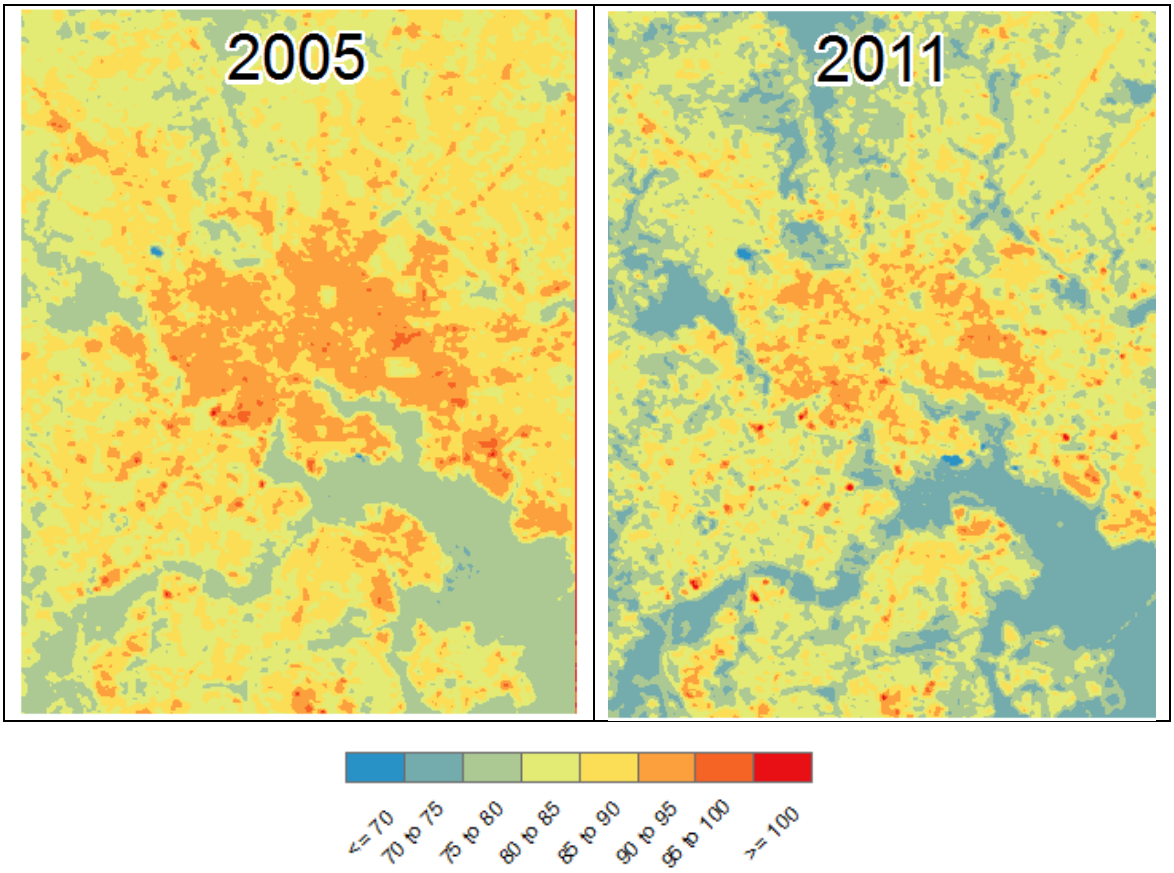

Figure 4.1. Land surface temperature maps (values are in ºF)

Changes in Land Surface Temperature 1985-2011

From 1985 to 1990 (Figure 4.3), the majority of the region appeared to have cooled between approximately 0Fº to -10Fº, with a mean of approximately -6.4Fº. The maximum cooling, or the minimum of the image, was -19.2Fº, while the maximum of the change image was +33.5Fº. Although the majority of the region cooled during the time period, there are a few spots of warming within the change image, though very sporadic. One of the notable hot spots, or spots of increased warming, is located in the northeastern corner of the image, along Route 1.

Between 1990 and 1996 (Figure 4.3), most of the study area increased in temperature, with several spots of cooling noted in the Patapsco River and towards the perimeter of the image, likely associated with deciduous forests. The downtown area appears to have increased between +5Fº to +10Fº, and in many areas more than +10Fº. As you move farther away from the downtown area, the increase in temperature decreases to between 0Fº to +5Fº; however increases between +5Fº to +10ºF are still seen along major roadways including Route 1 and I-95. The median value of the image is +5.6Fº, while the minimum is -10.8Fº, and the maximum is +43.9Fº.

Between 1996 and 2000 (Figure 4.3), cooling occurs again but not as severe as between 1985 and 1990. While the minimum cooling was -35.1Fº and the maximum warming was +25.4Fº, the majority of the area cooled between 0Fº to -5Fº, specifically between 0Fº and -2Fº. The mean of the image is a cooling of -1.3Fº.

Between 2000 and 2005 (Figure 4.3), there appears to have been some cooling towards the downtown / inner harbor area of Baltimore City, and several spots along major roadways. However, the majority of the region increased in temperature between 0Fº to +5Fº, with some areas increasing between +5Fº to +10Fº. Values in the image range from -25.4Fº to +25.1Fº with a mean of +3.4Fº.

Between 2005 and 2011 (Figure 4.3), the majority of the area cooled between -5Fº to 0Fº and -5 to -10Fº. Sparse areas of warming are noted throughout the image between 0Fº to +5Fº.

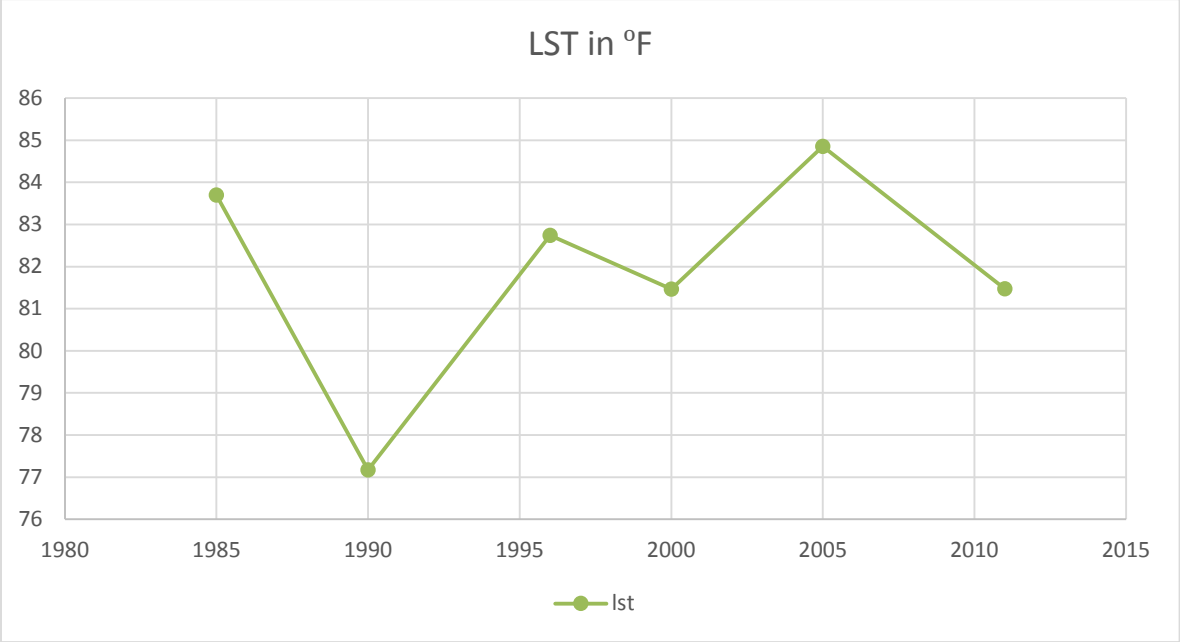

Figure 4.2. Average LST 1985-2011

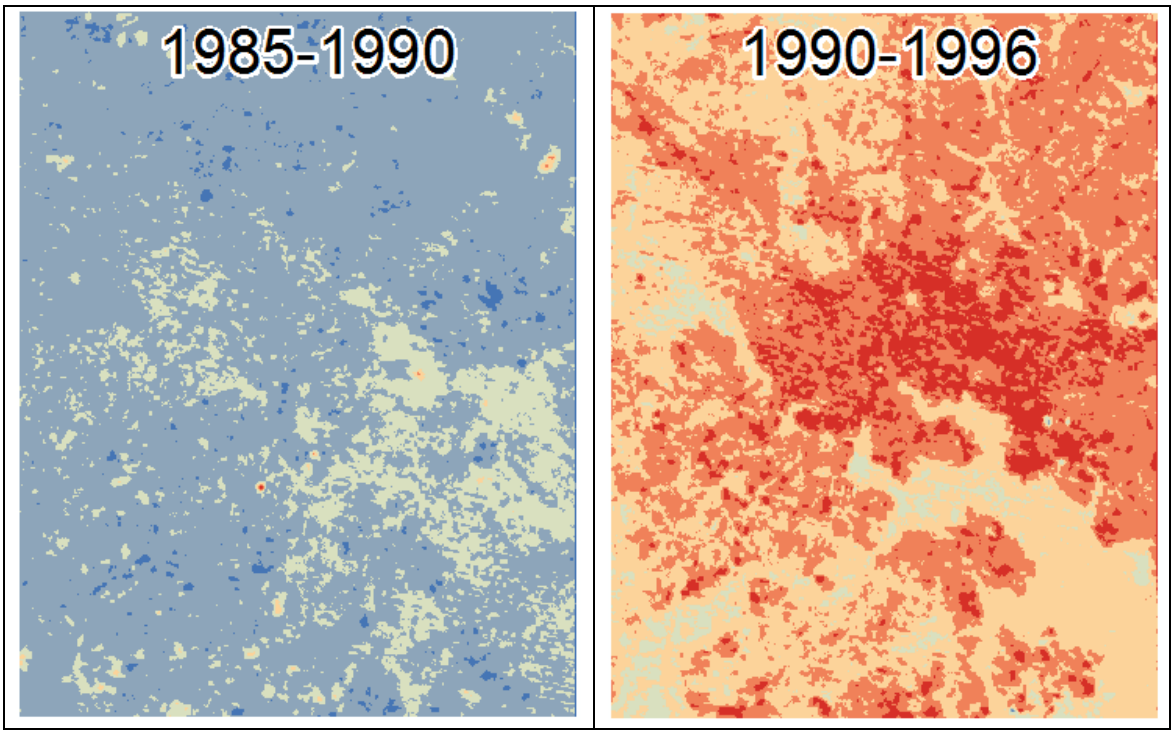

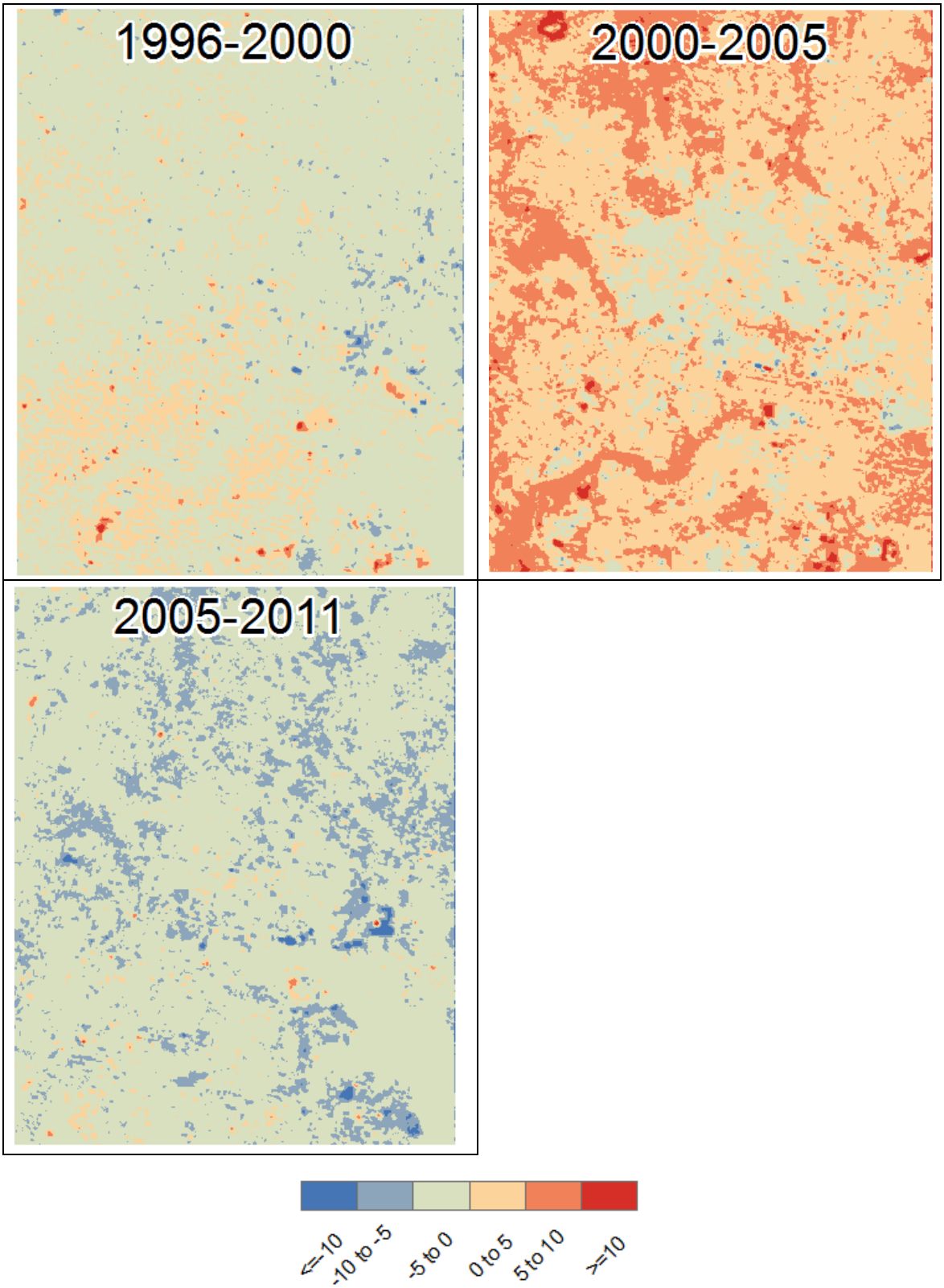

Figure 4.3. Land surface temperature change maps (values in F^{o})

Changes in Albedo 1985-2011 and Relationship to LST

Between 1985 and 1990 (Figure 4.5) the majority of the area decreased in albedo. Increases in albedo occurred primarily towards the western portion of Baltimore along roadways with some increases near the Patapsco River in the southeastern portion of Baltimore. The change in albedo and the change in LST during this time are not highly correlated, and have a coefficient *r* value of only -0.056 (Figure 4.6). This indicates a slightly negative relationship; however since the *r* value is so low, no real correlation can be extracted.

Between 1990 and 1996 (Figure 4.5), the overall albedo in the region decreased in value: 404,558 pixels decreased, while only 30,840 increased. Areas that increased appear to be located around the Patapsco River in the southeast, along with sporadic spots along major roadways extending outward from the downtown area. The change in albedo compared to the change in LST was not very correlated during this time (Figure 4.6), however this is the time period where they appear to be the most correlated as they had a coefficient *r* value of 0.413.

Between 1996 and 2000 (Figure 4.5), the region showed a relatively equal amount of increasing and decreasing pixels: 207,405 cells decreased in value and 227,993 increased in value. No clear pattern could be drawn from the increases and decreases as they appear to be mixed throughout the image. The regression model comparing the change in albedo and the change in LST indicates an *r* value of -0.554 (Figure 4.6). Therefore, the two variables are negatively related, however, they are not correlated enough to draw a conclusion on the relationship between the two.

Between 2000 and 2005 (Figure 4.5), the overall region increased in albedo: 408,841 cells increased, while only 26,557 pixels experienced a decrease. The decreases in albedo are seen mainly seen along major roadways, in sporadic parts of the downtown area, and surrounding the Patapsco River. Additionally, the linear regression between the change in albedo and the change in LST during this time, indicated an *r* value of 0.298 (Figure 4.6). This indicates a positive relationship during this time; however, the two variables do not appear to be very highly correlated.

Between 2005 and 2011 (Figure 4.5), the majority of the region decreased in albedo: 416,286 cells decreased, while only 19,112 cells increased. The mean albedo value in 2005 was 0.136 while it had been 0.098 in 2011. The regression model for this time period indicates an *r* value of only 0.036 (Figure 4.6). Therefore, the relationship between the change in albedo and the change in LST between 2005 and 2011, is positive, but overall not very highly correlated.

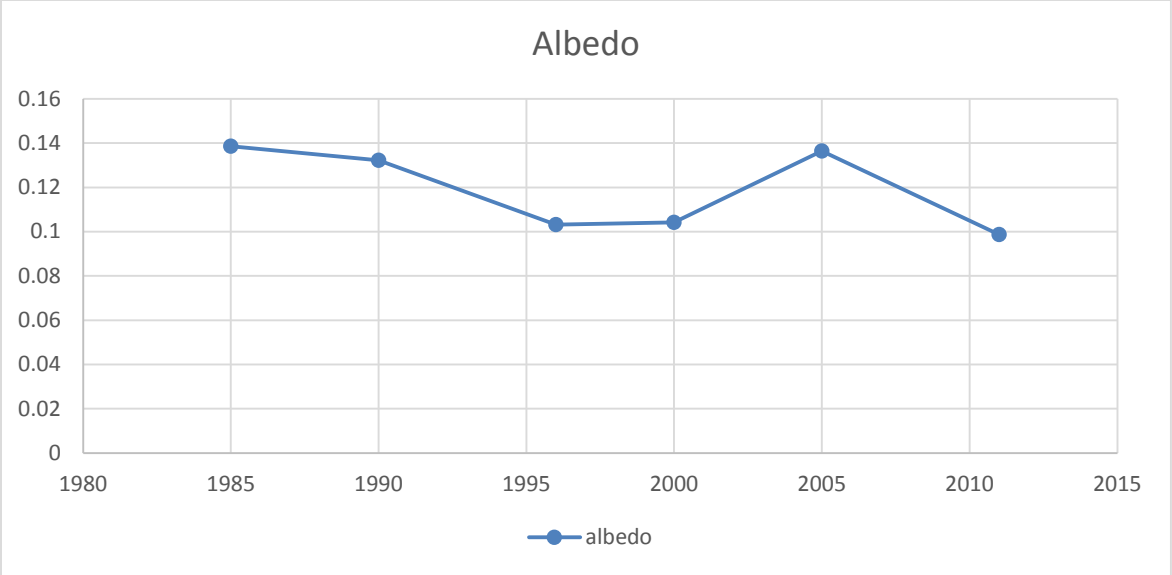

Figure 4.4. Albedo Values 1985-2011

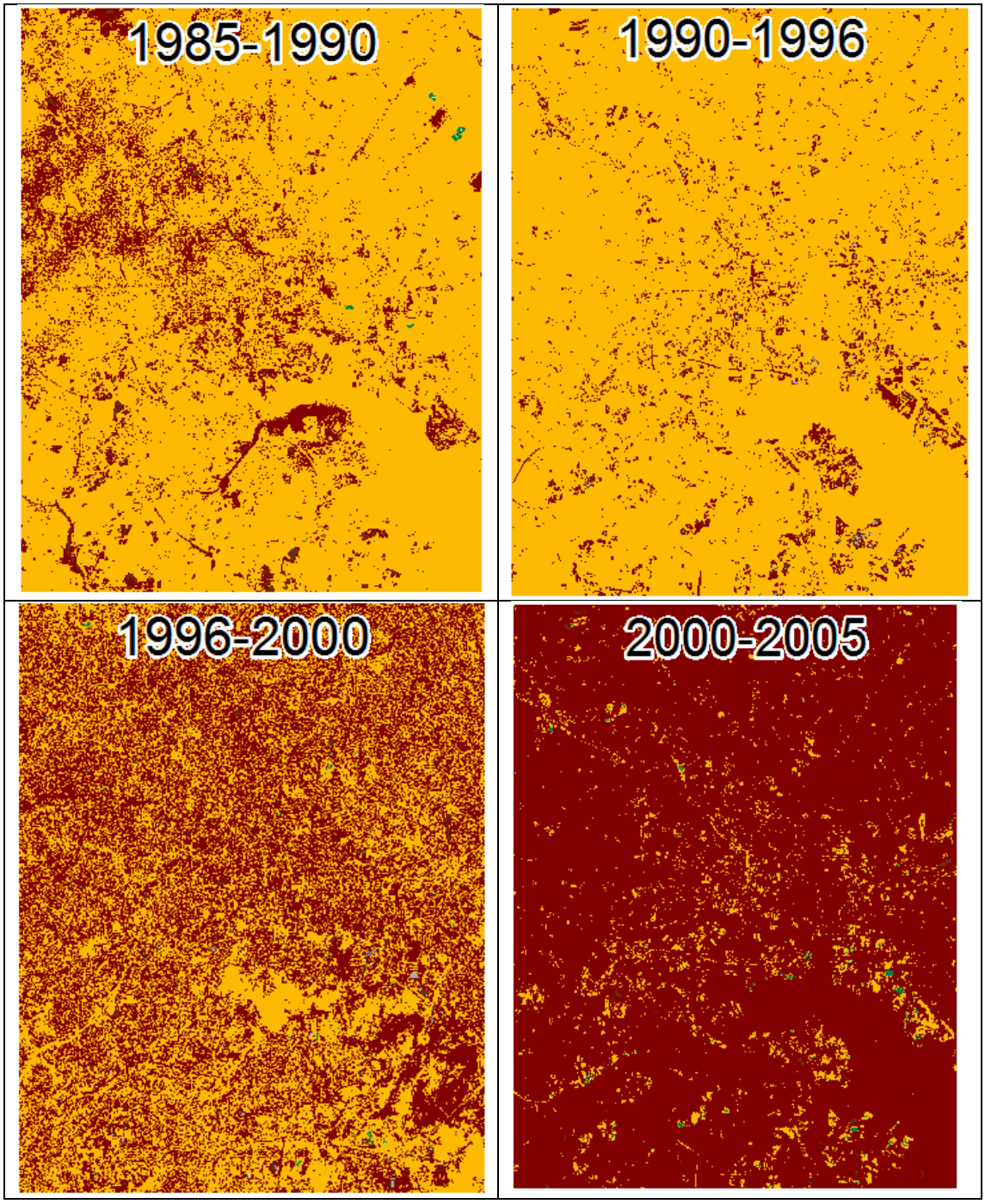
1985-1990
1990-1996
1996-2000
2000-2005

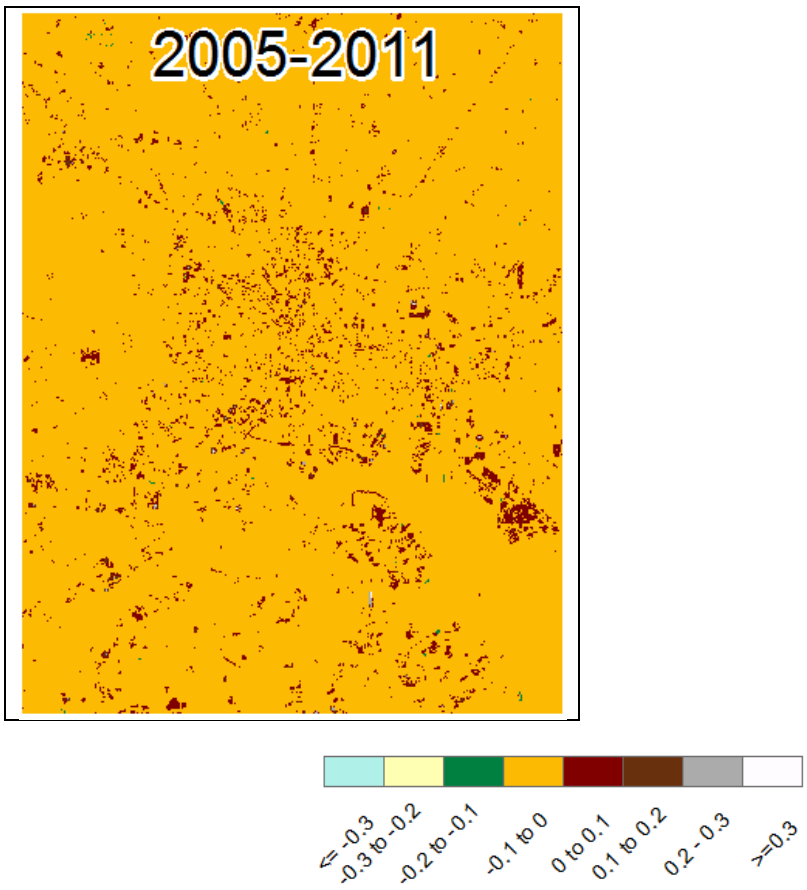

Figure 4.5. Albedo change maps

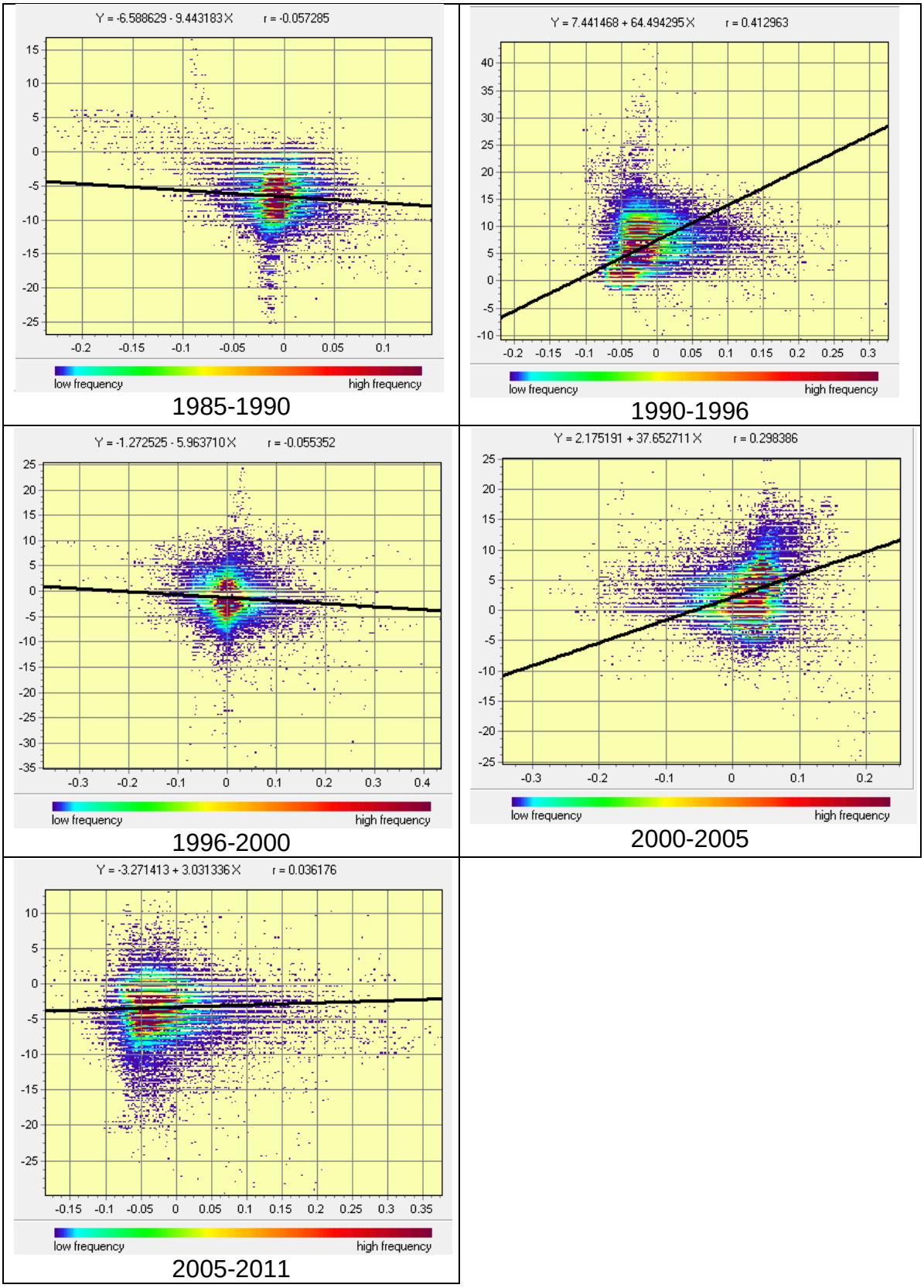

Figure 4.6. Albedo and LST regression analysis

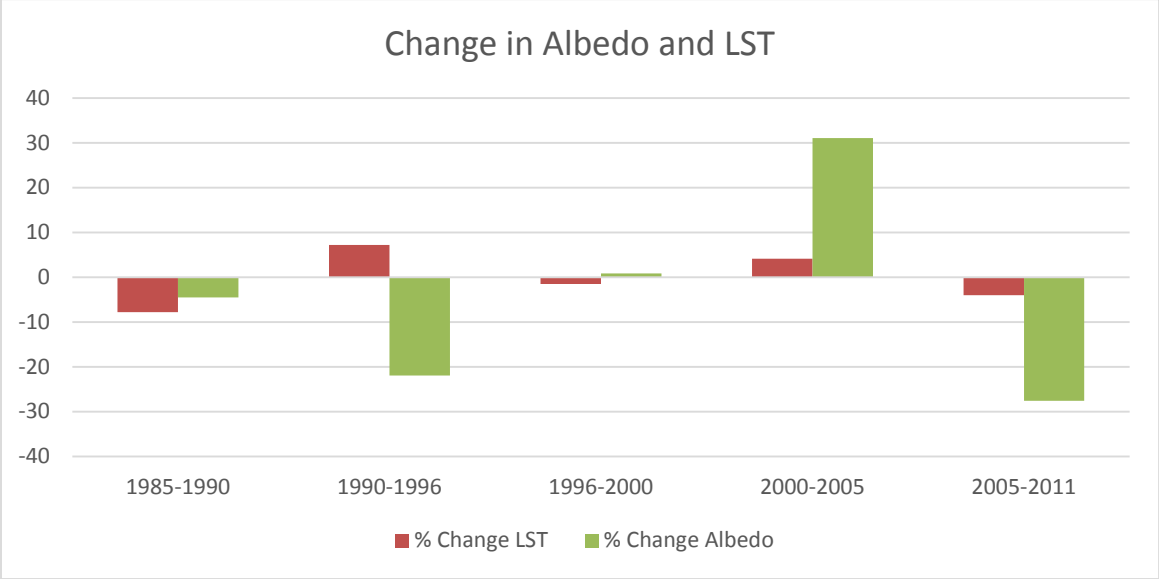

Figure 4.7. Change in Albedo and LST

Change in NDVI 1985-2011 and Relationship to LST

Between 1985 and 1990 (Figure 4.10) there was an overall increase in vegetation (or an increase in positive NDVI values); 314,021 pixels experienced an increase in NDVI while 121,377 decreased. Therefore, it appears there has either been an increase in the amount of vegetation, or existing vegetation has become healthier/greener. While the overall region increased, decreases are noted in the Patapsco River in the southeastern portion of the region, and along major roadways in the northeastern portion. The northwestern portion had a mixture of both increases and decreases, along with the southwestern portion. This time period is associated with a decrease in LST. Although not highly correlated, the *r* value for the regression between the change in NDVI and change in LST -0.278 (Figure 4.11).

Between 1990 and 1996 (Figure 4.10), there was also an overall increase in NDVI. Decreases are noted primarily where Patapsco River is located, in the southeastern portion of the region, however, other decreases are observed within the downtown portion of

Baltimore City and along major roadways. Some areas in the outskirts of the city also saw decreased NDVI values. This time period, just as the period before, saw a negative relationship between the change in NDVI and change in LST values (Figure 4.11). As NDVI increased, LST decrease. While the regression does not appear to be highly correlated, the *r* value of the regression was -0.330.

Between 1996 and 2000 (Figure 4.10), the NDVI values of the region appear to be mixed. Approximately half of the region become more vegetative and half became less vegetative. These values are mixed throughout the image and do not appear to fall into any specific pattern. The change in NDVI and the change in LST also reveals a negative correlation during this time. The regression analysis indicates an *r* value of -0.209 (Figure 4.11).

Between 2000 and 2005 (Figure 4.10), there appears to be less vegetation as more of the pixels decrease in values. Therefore either vegetation became more stressed or land surface changed. Oddly, areas that showed an increase in NDVI were located in the southeastern portion of the region (where the Patapsco River is located), in the downtown area, and along the roadways. This change was also associated with a negative correlation relative to change in LST. The regression indicated an *r* value of -0.471 (Figure 4.11). This time period showed the greatest negative correlation during the period's studies.

Between 2005 and 2011 (Figure 4.10), more pixels increased in value therefore becoming more positive, and more vegetative. This was primarily seen in the southeastern portion of the city (Patapsco River), and along major roadways. The water and areas surrounding the water as well, appeared to increase in NDVI values. The *r* value for the regression between NDVI and LST during this time was -0.279 (Figure 4.11).

Overall, the change in NDVI and change in LST maintained a negative correlation throughout the time studied. However, the two variables were not highly correlated, as the greatest *r* value is not much greater than -0.470.

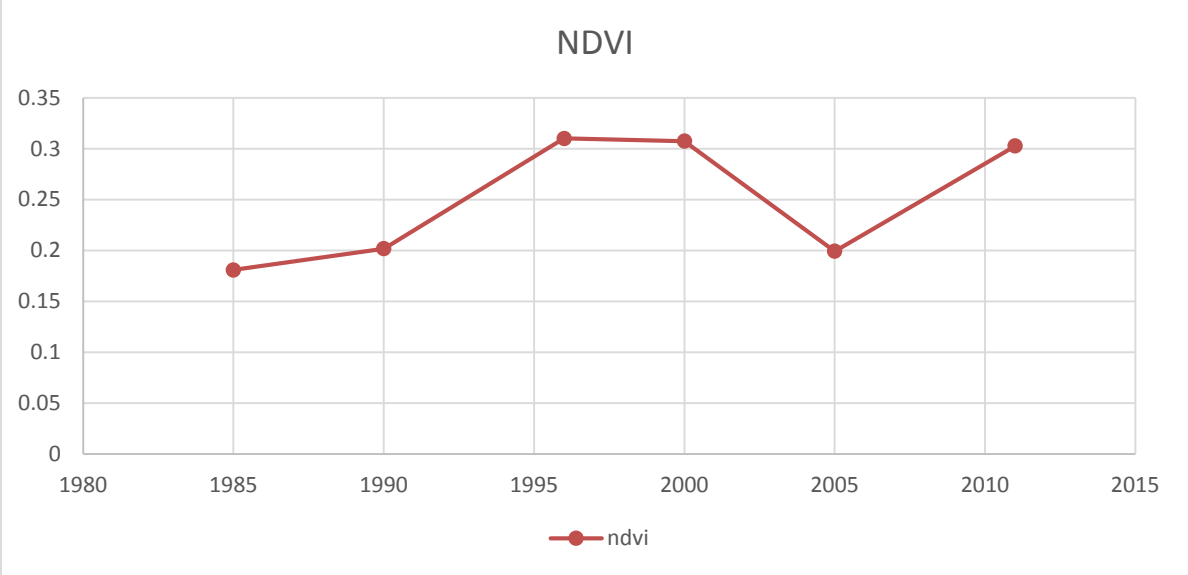

Figure 4.8. NDVI Values 1985-2011

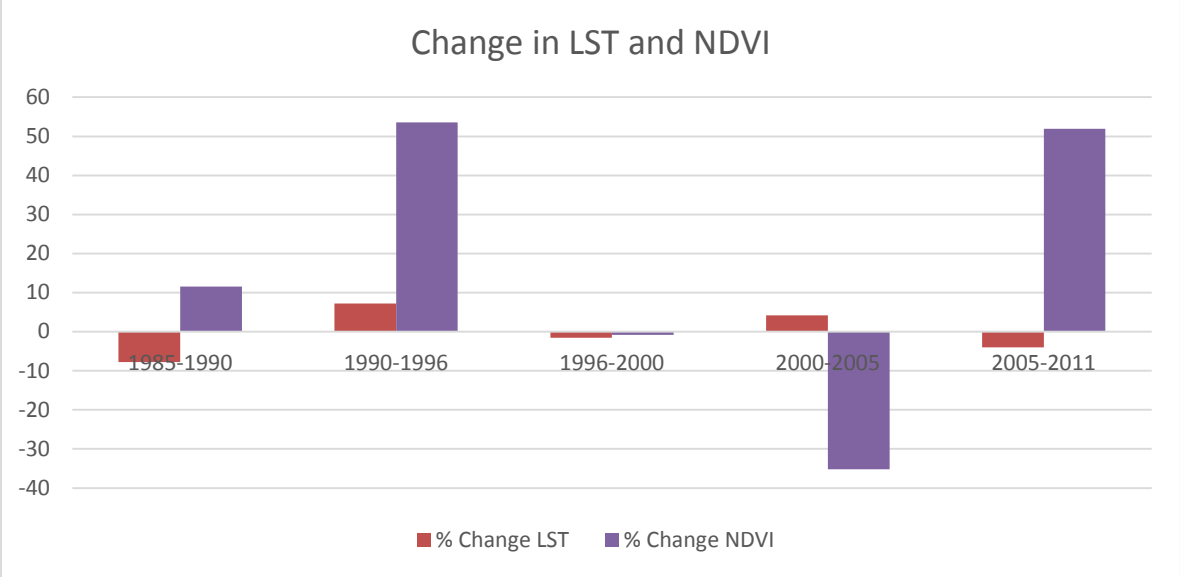

Figure 4.9. Change in LST and NDVI

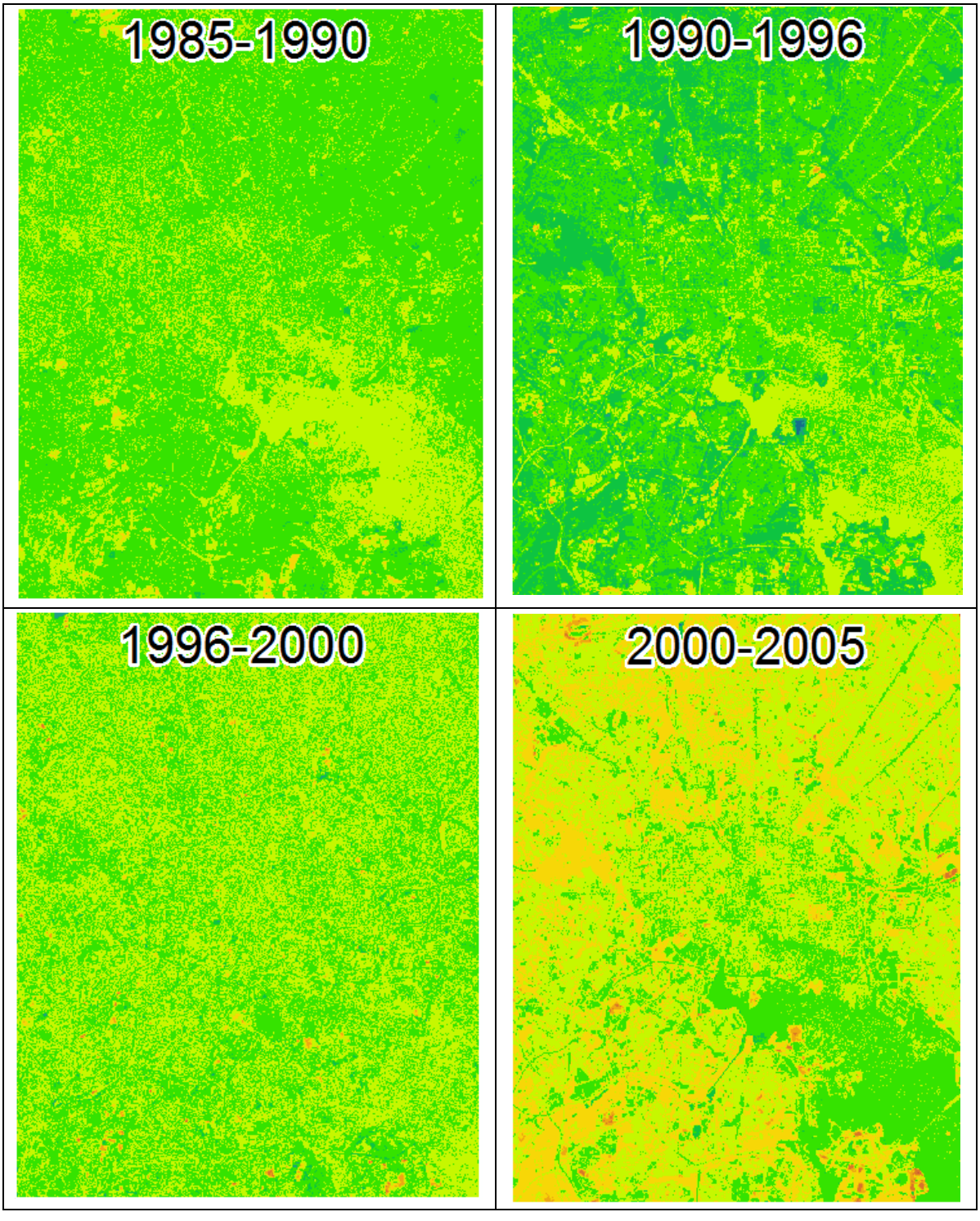
1985-1990
1990-1996
1996-2000
2000-2005

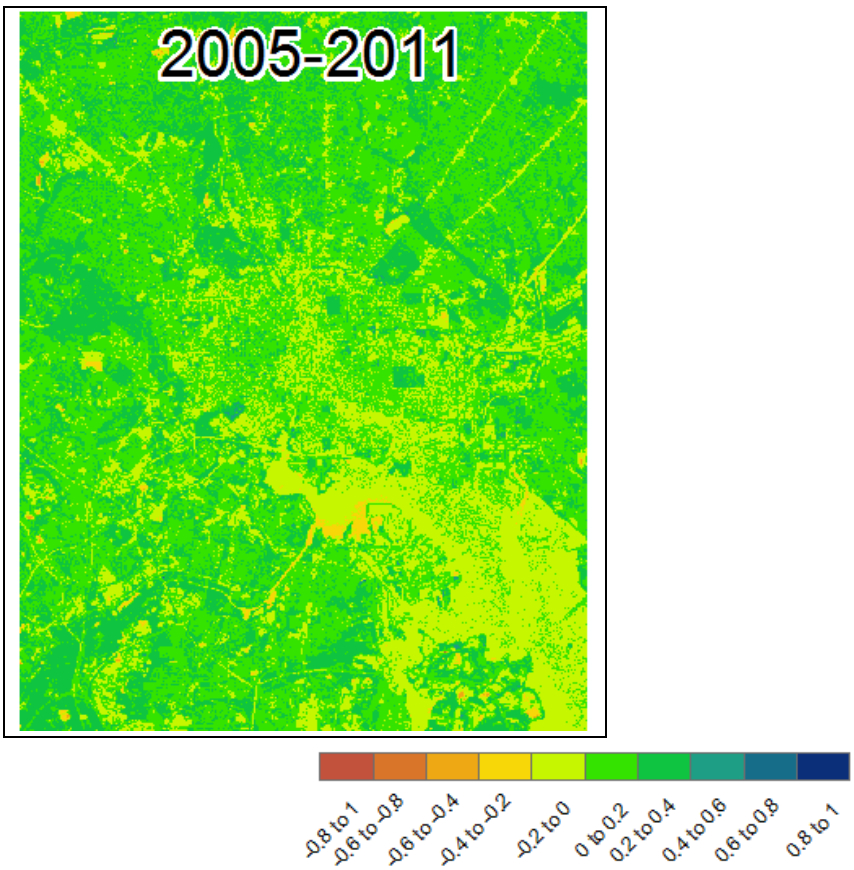

Figure 4.10. NDVI change maps 1985-2011

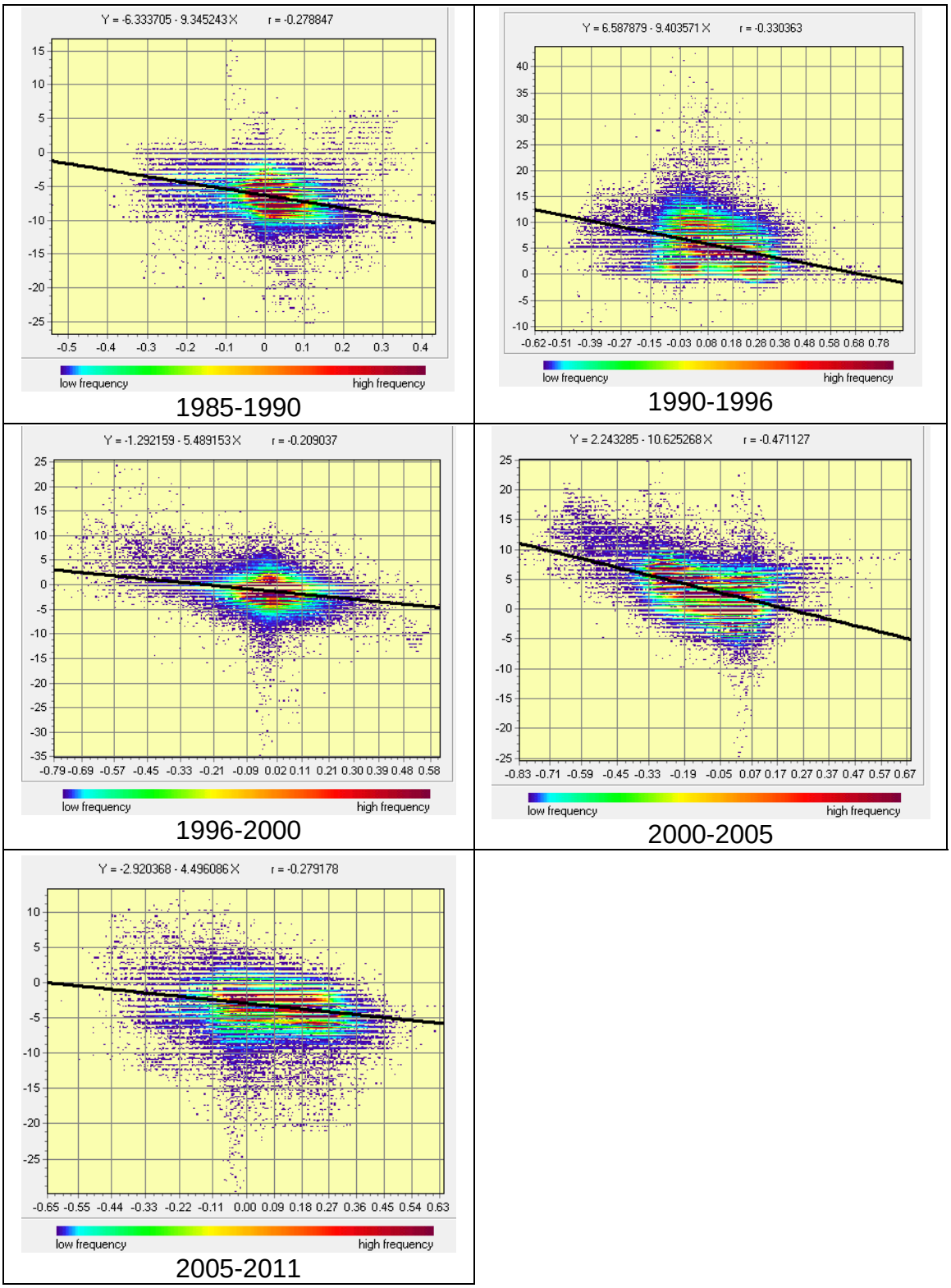

Figure 4.11. NDVI and LST regressions

Change in Land Cover and Relationship to LST

Land cover was classified into three groups: urban, non-urban, and water for the Baltimore City area. Land cover in the Baltimore area varied significantly between 1985 and 2011. Between 1985 and 1990 (Figure 4.12), urban land cover decreased approximately 5% going from 56% in 1985 to only 50% in 1990. This change appears to occur primarily in the east-northeastern portion of the city. Non-urban areas consequently increased during this time from 36% in 1985 to 42% in 1990. The decrease in urban land cover appears to occur in primarily in the northwestern portion of the city.

From 1990 to 1996 (Figure 4.12), urban land cover increased approximately 8.451% from 50% to 58%, while non-urban land cover decreased to approximately 32.771%. Much of this change appears to occur within the southwestern portion of the city and the northeastern portion. Between 1996 and 2000 (Figure 4.12), urban land cover decreased approximately 8% down to 50% in 2000, and then increased 4% up to 54% in 2005. Urban land cover decreased again approximately 4%, down to 50% in 2000. Non-urban areas increased from 33% to approximately 40% in 2000, but decreased to 37% in 2005. Non-urban areas increased to constitute 40% of land cover in 2011. The water land cover steadily decreased from 1985 to 2011. In 1985 water consisted of approximately 10% but only 7% of land cover in 2011 (Figure 4.12).

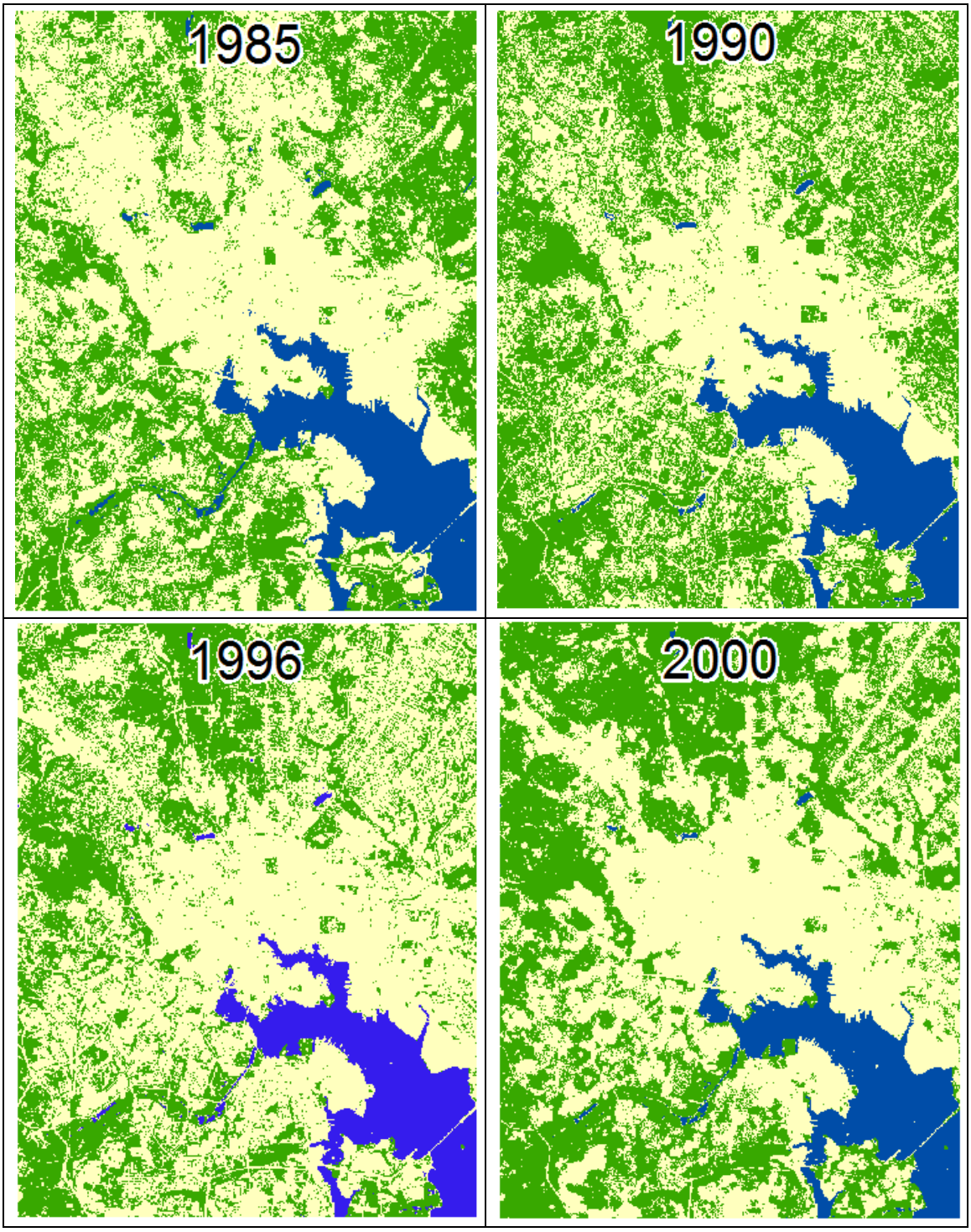
1985
1990
1996
2000

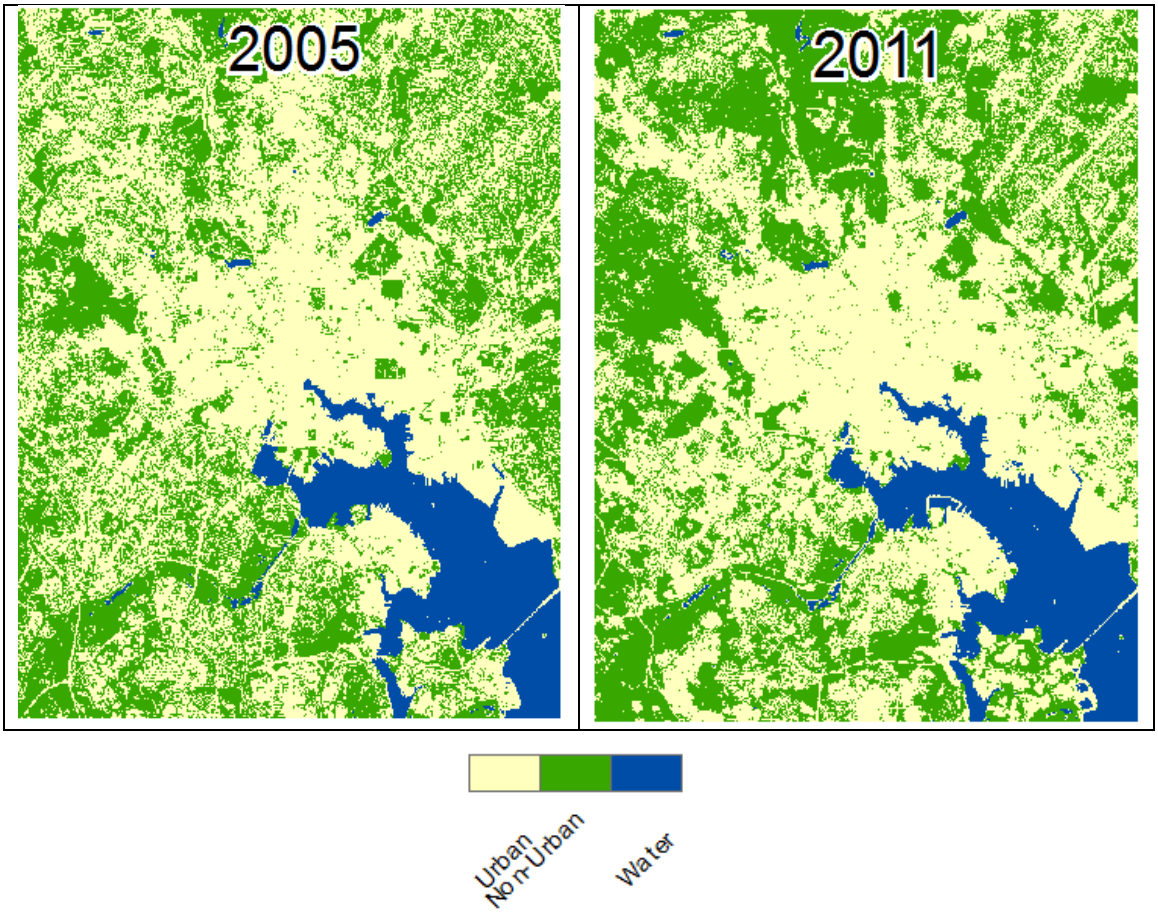

Figure 4.12. Land Cover Maps 1985-2011

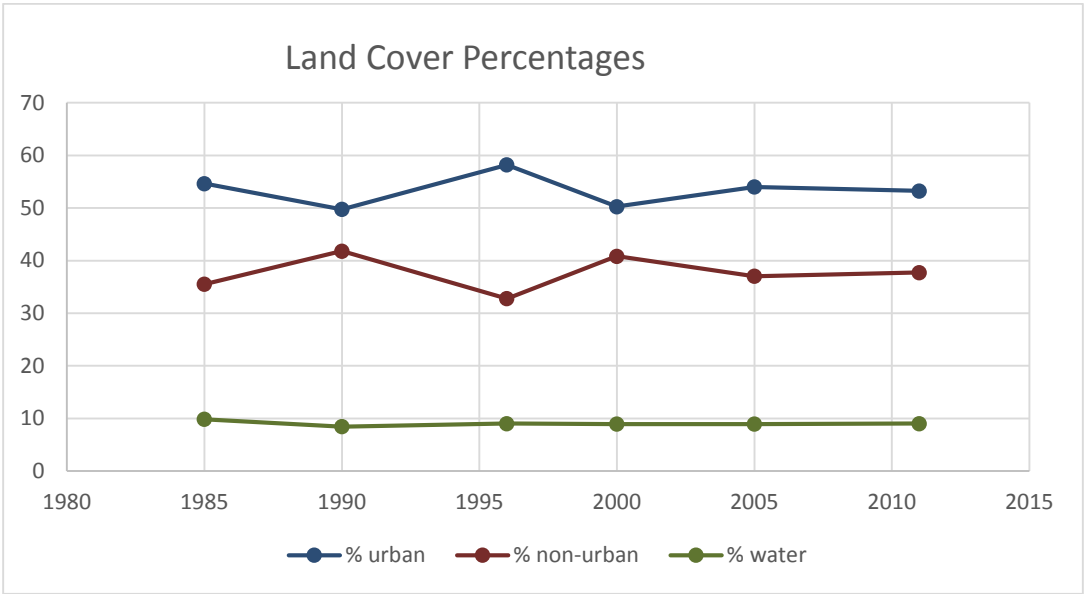

Figure 4.13. Land Cover Percentages 1985-2011

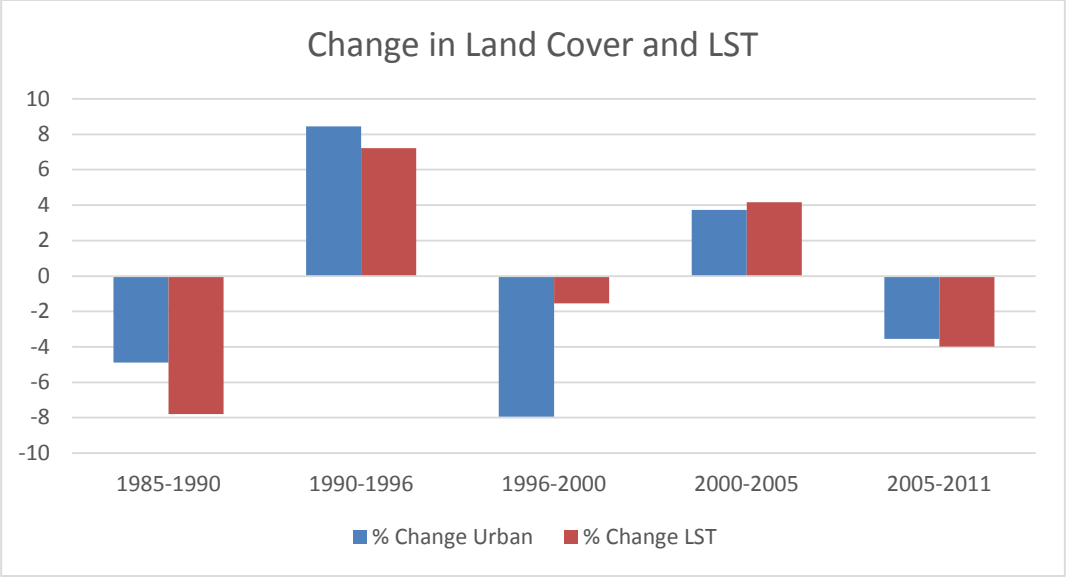

Figure 4.14. Change in Land Cover and LST 1985-2011

As shown in Figure 4.14, changes in land cover, specifically urban areas, appear to be highly correlated with changes in land surface temperature for the region and time period studied. Between 1985 and 1990, both urban areas and LST saw a decrease (first point on the figure), but then increased between 1990 and 1996. Both variables decreased between 1996 and 2000, and increased between 2000 and 2005. Percentage of urban areas and LST decreased between 1995 and 2000 and increased between 2000 and 2005. Between 2005 and 2011, there was a slight decreased in both urban areas and LST. Overall, the change in urban areas coincide with a change in LST. A positive changes, such as between 1985 and 1990 corresponds to a positive change or increase in LST, while a decrease in the change of urban areas also corresponds to a decrease in the change in LST. It should be noted that some differences in change could be a result of the automatic clustering within ISOCLUST, along with the manual aggregation of the categories within the land cover classification.

CHAPTER 5

DISCUSSION

The LST change maps for Baltimore's UHI between 1985 and 2011 show that LST cooled and warmed between the images. It is unlikely that Baltimore's UHI went away between 1985-1990, 1996-2000, and 2005-2011, but then rematerialized between the other years. The changes in land cover from urban to non-urban were unlikely to force the cooling that took place during these time periods. Albedo and NDVI also did not change in such a way to force these changes in LST (Figure 4.7 and 4.9). Therefore, other factors are likely to have influenced LST. One possibility includes the weather present before and on the day the image was taken, particularly precipitation.

The Potential Role of Weather and Precipitation

Preceding precipitation events could cause cooling if it occurred prior to the later image but not the prior to the other one. Precipitation would increase the latent heat flux and reduces the sensible heat flux, thereby reducing LST. To determine if this was a possibility, data was collected from the United States Historical Climatology Network (USHCN) for all of the images (Figure 5.1).

A look at the precipitation data between 1985 and 1990 indicates that some of the cooling within this time period may be attributed to the precipitation events that occurred in the days prior to the 1990 image along with the absence of precipitation in the days leading up to the 1985 image (Figure 5.1). Nearly 2 inches (in.) of precipitation occurred on August 6, 1990, with two more inches occurring on August 9 and August 10, 1990 collectively. Some of the warming between 1990 and 1996 may also be attributed to the

precipitation events that occurred prior to the 1990 image along with absence of heavy rain fall prior to the 1996 image (Figure 5.1).

The cooling that took place between 1996 and 2000 may be also associated with the minor precipitation event that occurred the day before the 2000 image captured along with the approximately 0.75 in. of rain that occurred two days prior (Figure 5.1).

Precipitation fell on the day the 2005 image was captured (Figure 5.1). However, according to information obtained from NASA's North American Land Data Assimilation System (NLDAS), precipitation occurred hours after the image was captured.

The overall cooling of the area between 2005 and 2011 is likely associated with the heavy amount of precipitation that occurred prior to the 2011 image (Figure 5.1). In the ten days prior to the image, approximately 7 in. of rain occurred, with almost 2 in. of rain occurring the day before the image was captured.

To further illustrate the possible influence of precipitation on the change in UHI, LST change maps for 1985 and 2009, and 1985 and 2011 were created. It is unlikely that the morphology of Baltimore's UHI changed substantially between 2009 and 2011. These two images, however, do have different precipitation amounts preceding their capture. The 2009 image had no precipitation in the five days prior to the date of image capture, while the 2011 had approximately 7 in. of rain in the ten days leading up to the image (Figure 5.1.).

Between 1985 and 2009 (Figure 4.3), the majority of the image increased in temperature between 0F^{o} to +5F^{o}, with some areas, particularly the downtown area and the eastern portion of Baltimore City increasing between +5F^{o} to +10F^{o}. Values in the image range from -30.8F^{o} to +32.6F^{o} with a mean of +1.7F^{o}. Cooling in the image occurred in the

Patapsco River to the southeast of the image, and in forested areas in the southwestern and western portion of Baltimore City. Sporadic hot spots of greater than +10Fº are noted throughout the image, particularly in the downtown area but also near the southern and southwestern border of the study area.

Between 1985 and 2011, the majority of the image cooled between 0Fº and -5Fº and -5Fº to -10Fº. Values in the image range from -40.1Fº to +22.9Fº with a mean of -2.2Fº. Some areas of warming of 0Fº to +5Fº are noted within the image, primarily in the downtown area and along major roadways. Some sporadic hotspots are noted throughout the southern portion of the image.

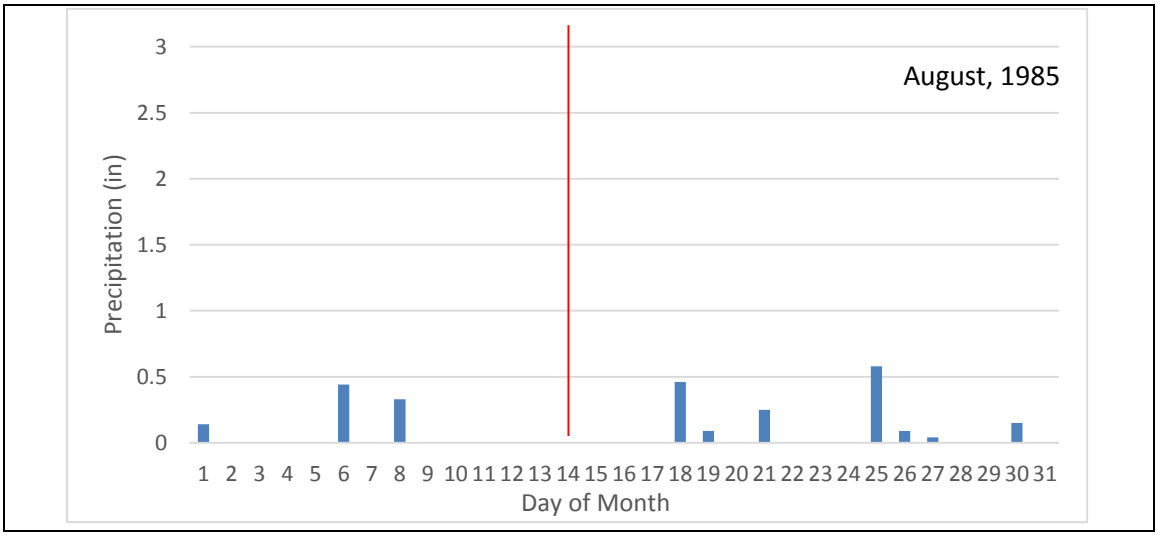

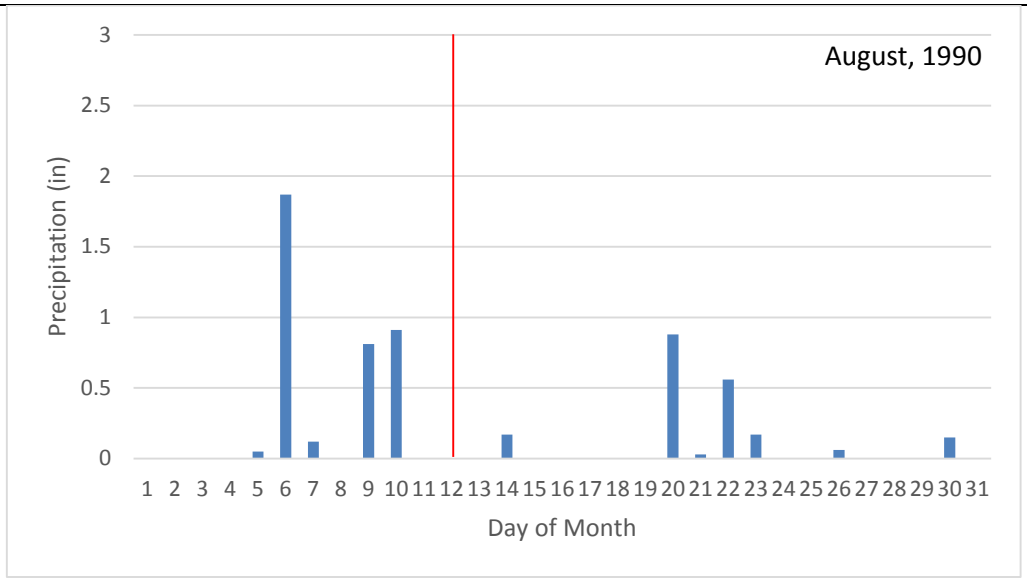
August, 1990
Precipitation (in)
3
2.5
2
1.5
1
0.5
0
1 2 3 4 5 6 7 8 9 10 11 12 13 14 15 16 17 18 19 20 21 22 23 24 25 26 27 28 29 30 31
Day of Month

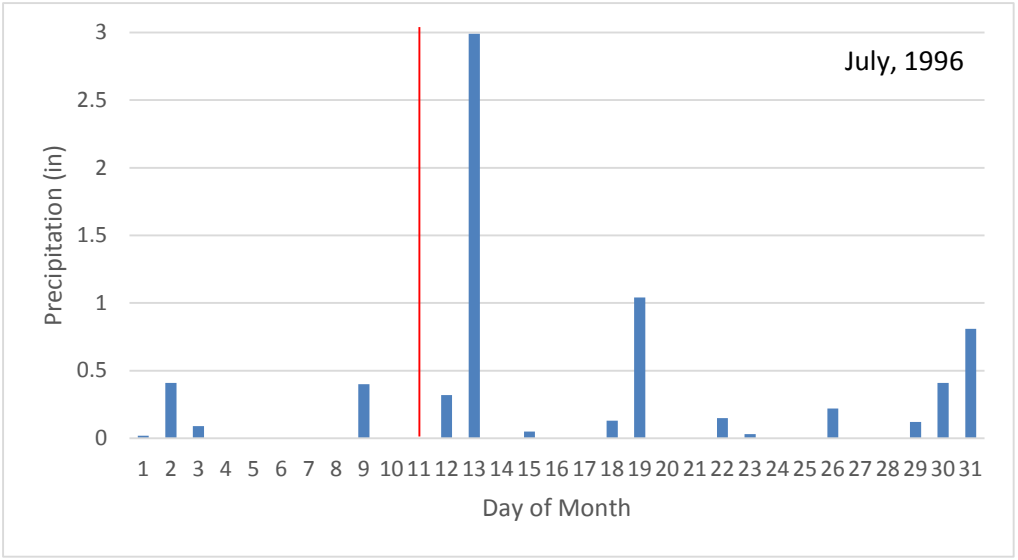
July, 1996
Precipitation (in)
3
2.5
2
1.5
1
0.5
0
1 2 3 4 5 6 7 8 9 10 11 12 13 14 15 16 17 18 19 20 21 22 23 24 25 26 27 28 29 30 31
Day of Month

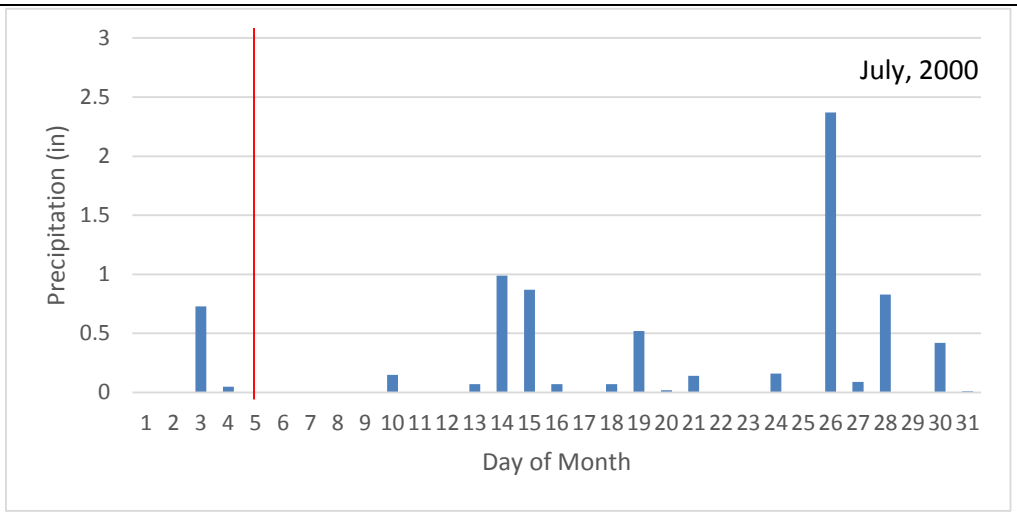
July, 2000
Precipitation (in)
3
2.5
2
1.5
1
0.5
0
1 2 3 4 5 6 7 8 9 10 11 12 13 14 15 16 17 18 19 20 21 22 23 24 25 26 27 28 29 30 31
Day of Month

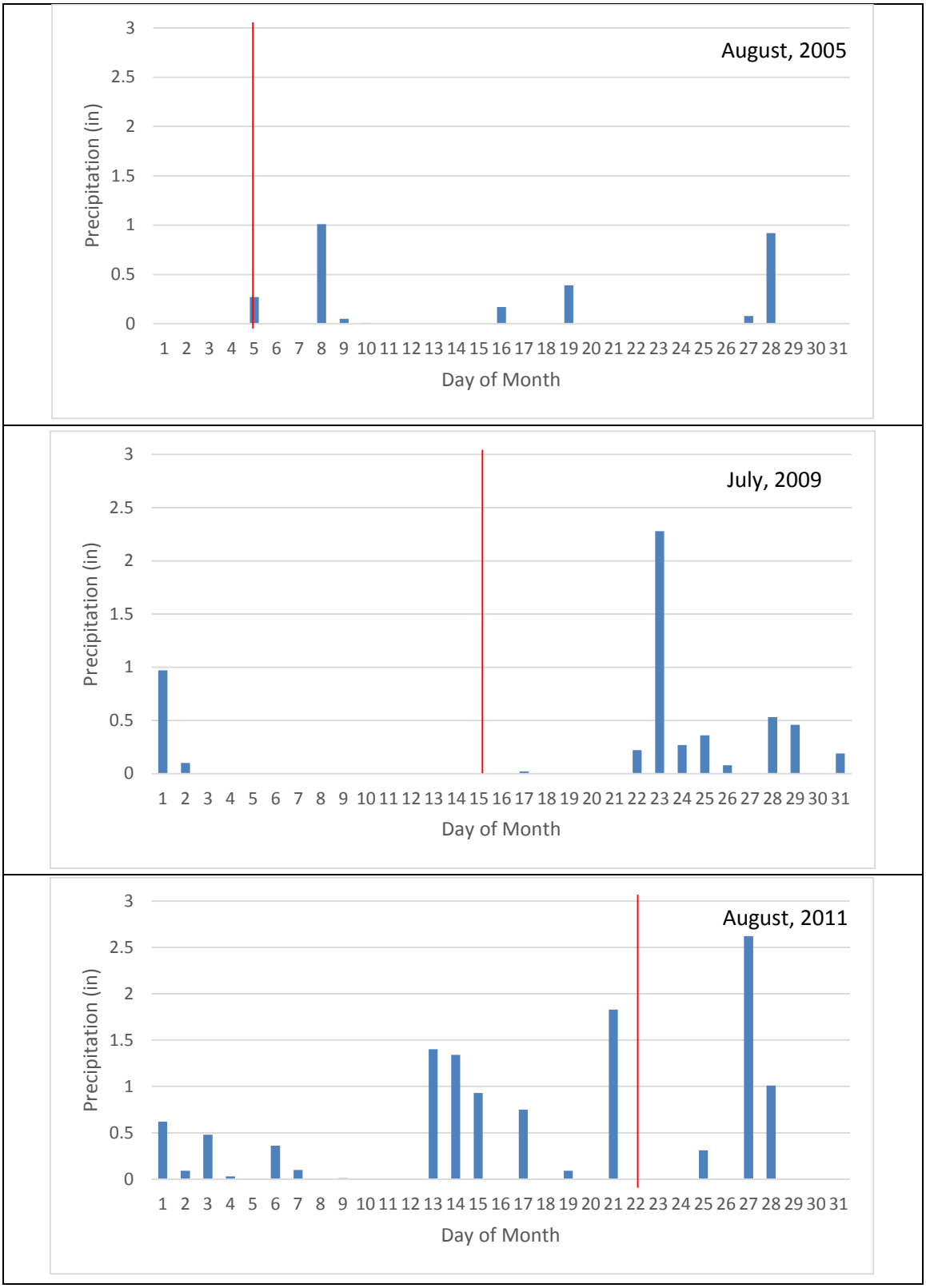

Figure 5.1. Climate Data. Sources: United States Historical Climatology Network, Version 2.

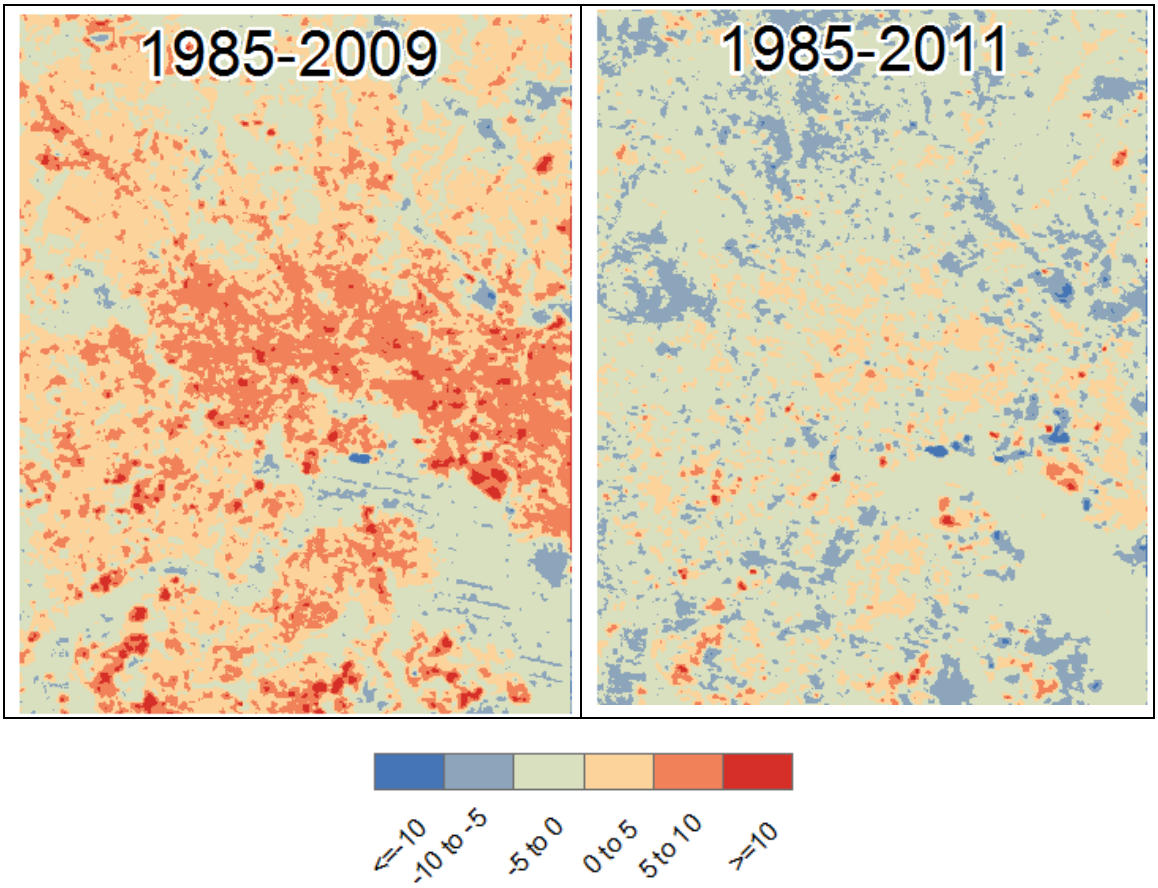

Figure 5.2. LST change maps 1985-2009 and 1985-2011 (values in F°)

Recommendations and Further Studies

Further studies are needed in order to fully utilize and understand the results of this study. Weather, particularly precipitation events, appears to have convoluted the extent and intensity of Baltimore's UHI in this study. Precipitation events may have masked the UHI effect when the events occurred prior to the later image capture date as in the case between 1985 and 1990. Precipitation events may have also created an apparent intensification of the UHI when they occurred prior to the earlier image as shown between 1990 and 1996. The precipitation events also may affect LST and other surface properties (e.g., albedo and NDVI) differently. If so, this may have contributed to the weak correlations observed between changes in LST and changes surface properties (i.e., albedo and NDVI).

The relationship between water/moisture content of surfaces and UHIs is beginning to be studied (Hendel *et al.*, 2015; Higashiyama *et al*, 2016). Hendel *et al.*, (2015), for instance, focuses on watering pavement as a potential climate change adaptation method. The study found that watering pavement lowered LST for pavement surfaces by several degrees for a few hours after watering and reduced the cooling rate for several hours before and after sunset. The study also found that heat flux and storage of the pavement were significantly reduced to a depth of about 2 in. (5 centimeters), "resulting in negative storage balance for watered day (Hendel *et al.*, 2015, 10)."

CHAPTER 6

CONCLUSIONS

This study sought to map the change and extent of Baltimore's UHI. This relied on the use of remotely sensed data and digital image processing software, TerrSet, to execute change detection. Change for the area was determined based on changes in land cover, and the extent and intensity of Baltimore's UHI. This was done through the extraction of LST and the extraction of albedo, NDVI, and land cover for images dated 1985, 1990, 1996, 2000, 2005, and 2011. This study focused on the change in albedo, NDVI, land cover, and LST, and the correlation between the changes in albedo, NDVI, and land cover on LST. The results of this analysis add to knowledge for future studies on the impacts on LST as a result of changes in albedo, NDVI, and land cover.

Important Findings

This study revealed an association between the change in land cover and change in LST for the Baltimore region between 1985 and 2011. Increases in the percentage of urban land cover for the region were associated with increases in LST, while decreases in the percentage of urban land cover for the region were associated with decreases in LST. Changes in albedo and NDVI, however, were revealed to not be highly correlated with changes in LST. These weak correlations might be the result of the precipitation events influencing the variables differently.

Although changes in land cover appeared to be associated with changes in LST, they were not enough to force the changes that occurred in LST. This analysis revealed an approximately -6.5F^{o} decrease in LST from 1985 to 1990, and overall increase of approximately +4.3F^{o} between 1990 and 2011. Slight decreases occurred from 1996 to

2000 and from 2005 to 2011, some of which is likely the result of precipitation events that occurred prior to the images. For instance, the decrease between 2005 and 2011 may be associated with precipitation event that occurred a few days prior to the date of the Landsat 5 imagery. This appears to have resulted in an inverse relationship of the UHI, in which urban areas appeared to have decreased, while vegetated areas, appear to have still increased in LST during that time.

Because of this, LST change between 1985 and 2009 and between 1985 and 2011 was also looked at in order to illustrate the role of precipitation events on LST. This comparison showed that the precipitation events that occurred prior to the 2011 image resulted in a decrease in overall LST in Baltimore's UHI, while when there was no precipitation (as in the 2009 image), LST increased.

The findings of this study can be used by policymakers and planners in order to make strategic decisions regarding development, specifically urban development. The findings of this study can also be used for education and public outreach to exemplify the effects of UHIs and draw connections on human alterations and global climate change. Future research will need to done in order to fully utilize the results of this study and determine if the results hold true over other urban environments.

Limitations of the Study

The goal of this project was to analyze the change and extent of Baltimore's UHI, and to analyze the associations between changes in surface properties (i.e., albedo, NDVI, and land cover) and changes in LST. Data downloaded from the USGS EarthExplorer website consisted of Landsat 5 imagery, which consists of 30 meter resolutions for all bands except for Band 6, which is 120 meters in resolution. Therefore, spatial and spectral

resolution of the images were limited. Additionally, the images, although taken on anniversary dates were not taken at the exact same time of the year and not all of the data was available, cloud free, in 5 year intervals. Weather and precipitation events leading up to the imagery dates may have also played a role in part of the changes in albedo, NDVI, land cover, and LST, as noted for the 2011 image.

Another limitation is that ISOCLUST was performed with only ten cluster classes. Ten classes were chosen in order to effectively determine urban areas versus the non-urban and water areas. Utilizing more clusters may have resulted in more accurate land cover classes; however it would have also allowed for more manual error, or misclassification, during aggregation.

BIBLIOGRAPHY

Ahmed, Bayes, Md Kamruzzaman, Xuan Zhu, Md Shahinoor Rahman, and Keechoo Choi. "Simulating land cover changes and their impacts on land surface temperature in Dhaka, Bangladesh." *Remote Sensing* 5, no. 11 (2013): 5969-5998.

Baltimore Commission on Sustainability, and Baltimore City Planning Commission. "The Baltimore Sustainability Plan." (n.d.): n. pag. Apr. 2009. Web. 22 Nov. 2015.

Bhamare, S. M., and Vikram Agone. "Change Detection of Surface Temperature and its Consequence Using Multi-Temporal Remote Sensing Data and GIS Application to Tapi Basin of India." (1990).

Chen, Xiao-Ling, Hong-Mei Zhao, Ping-Xiang Li, and Zhi-Yong Yin. "Remote sensing image-based analysis of the relationship between urban heat island and land use/cover changes." *Remote sensing of environment* 104, no. 2 (2006): 133-146.

Effat, Hala Adel, and Ossman Abdel Kader Hassan. "Change detection of urban heat islands and some related parameters using multi-temporal Landsat images; a case study for Cairo city, Egypt." *Urban Climate* 10 (2014): 171-188.

George, Linda Acha, and William G. Becker. "Investigating the urban heat island effect with a collaborative inquiry project." (2003).

Grimmond, Oke, T., 1991. An evapotranspiration-interception model for urban areas. Water Resour. Res. 27, 1793.

Hendel, M. A., Colombert, M., Diab, Y., Royon, L., Measurement of the Cooling Efficiency of Pavement-watering as an Urban Heat Island Mitigation Technique, J. sustain. dev. energy water environ. syst., 3(1), pp 1-11, 2015, http://dx.doi.org/10.13044/j.sdewes.2015.03.0001

Higashiyama, Hiroshi, Masanori Sano, Futoshi Nakanishi, Osamu Takahashi, and Shigeru Tsukuma. "Field measurements of road surface temperature of several asphalt pavements with temperature rise reducing function." *Case Studies in Construction Materials* (2016).

Liu, L; Zhang, Y. “Urban heat island analysis using the Landsat TM data and ASTER data: A Case study in Hong Kong.” *Remote Sens.* 2011, *3*, 1535–1552.

Lo, Chor Pang, Dale A. Quattrochi, and Jeffrey C. Luvall. "Application of high-resolution thermal infrared remote sensing and GIS to assess the urban heat island effect." *International Journal of Remote Sensing* 18, no. 2 (1997): 287-304.

Ma, Ya, Kuang, Y., Huang N., 2010. Coupling urbanization analysis for studying urban thermal environment and its interplay with biophysical parameters based on TM/ETM_ imagery. Int. J. Appl. Earth Obs. Geoinf. 12, 110-118.

Morgan, John. “Lecture 1.” GEOG674 Remote Sensing. Towson University, Towson. 2014. Lecture.

National Air and Space Administration. "Measuring Earth’s Albedo: Image of the Day." *Measuring Earth’s Albedo: Image of the Day*. Web. 13 Nov. 2015.

Nesarikar-Patki, P; Raykar-Alange, P. “Study of Influence of Land Cover on Urban Heat Islands in Pune Using Remote Sensing.” *ISOR Journal of Mechanical and Civil Engineering.* 39-43.

Oke, T.R., 1982. The energetic basis of the urban heat island. Q. J. R. Meteorol. Soc. 108, 1–24.

Oke, T.R., 1995. The heat island of the urban boundary layer: characteristics, causes and effects. In: Cermak, J.E., Davenport, A.G., Plate, E.J., Viegas, D.X. (Eds.), Wind Climate in Cities. Kluwer Academic, Dordrecht, pp. 81–107.

Rinner, C.; Hussain, M. Toronto’s urban heat island- Exploring the relationship between land use
and surface temperature. *Remote Sens.* **2011**, *3*, 1251–1265.

Sobrino, J.A.; Jimenez-Munoz, J.C.; Paolini, L. “Land surface temperature retrieval from LANDSAT TM 5.” *Remote Sens. Environ.* 2004, *90*, 434-440.

Stathopoulou, M.; Cartalis, C; Andritsos, A. "Assessing the thermal environment of major cities in Greece." In *Proc. 1st International Conference on Passive and Low Energy Cooling for the Built Environment, Santorini, Greece*. 2005.

Voogt, J.A., Oke, T.R., 1997. Complete urban surface temperatures. J. Appl. Meteorol. 36, 1117–1132.

Voogt, J.A., Oke, T.R., 2003. Thermal remote sensing of urban climates. Remote Sens. Environ. 86, 370–384.

Weng, Qihao. "Fractal analysis of satellite-detected urban heat island effect." *Photogrammetric engineering and remote sensing* 69, no. 5 (2003): 555-566.

Zhang, Z., M. Ji, J. Shu, Z. Deng, and Y. Wu. "Surface Urban Heat Island In Shanghai, China: Examining The Relationship Between Land Surface Temperature And Impervious Surface Fractions Derived From Landsat ETM+ Imagery." *The International Archives of the Photogrammetry, Remote Sensing and Spatial Information Sciences* 37 (2008): 601-606

CURRICULUM VITA

NAME: Sara H. Levy
PERMANENT ADDRESS: 2406 Forest Green Road, Baltimore, MD 21209
PROGRAM OF STUDY: Geography and Environmental Planning
DEGREE AND DATE TO BE CONFERRED: Master of Arts, 2016

Secondary education: Owings Mills High School, Owings Mills, MD. 21117

Collegiate institutions attended:
University of Maryland, College Park, MD. 2010-2013. Bachelor of Science. 2013
Major: Environmental Science and Policy

Towson University, Towson, MD. 2013-2016. Master of Arts. 2016
Major: Geography and Environmental Planning

Professional positions held:
2015-Present. Project Scientist II. Trileaf Corporation. 8600 LaSalle Road, Suite 301, Towson, MD 21286.

2013-2016. Staff Scientist. Advantage Environmental Consultants, LLC. 8610 Washington Boulevard, Suite 217, Jessup, MD 20794.

2013. Administrative Assistant. Park Medical Associates. 10755 Falls Road, Lutherville, MD 21093.

2012. Intern. National Oceanic and Atmospheric Administration. 1315 East-West Highway, Silver Spring, MD 20910.